Annu. Rev. Earth Planet. Sci. 1995. 23:169–213
Copyright © 1995 by Annual Reviews Inc. All rights reserved

ANNUAL REVIEWS Further
Quick links to online content

THE MECHANICS OF DEEP EARTHQUAKES

Harry W. Green II

Institute of Geophysics and Planetary Physics and Department of Earth Sciences, University of California, Riverside, California 92521

Heidi Houston

Institute of Tectonics, University of California, Santa Cruz, California 95064

KEY WORDS: anticrack, dehydration, embrittlement, phase transformations, seismology, subduction

Annu. Rev. Earth Planet. Sci. 1995.23:169-213. Downloaded from www.annualreviews.org
by California Institute of Technology on 06/20/13. For personal use only.

INTRODUCTION

A wide variety of experimental and observational data demonstrate that shallow earthquakes are the result of either brittle shear failure during creation of a fault or stick-slip friction on a preexisting fault (cf Scholz 1990). The same experimental data that yield understanding of this process, however, show that such frictional processes are strongly inhibited by temperature and pressure. Under any specified set of environmental conditions, failure can occur, in principle, by either flow or fracture. The flow stress of rocks is strongly reduced by increasing temperature because motion of crystal dislocations is thermally activated, whereas flow processes are essentially unaffected by pressure. Fracture and frictional processes, on the other hand, are strongly inhibited by pressure because they involve the opening of tensile microcracks, but are not affected strongly by temperature. Because increasing temperature and pressure both favor flow, earthquakes caused by frictional mechanisms become impossible below a depth of about 30 km along a normal geotherm, unless some additional factor is involved. Indeed, in most geological environments, earthquakes below 30 km are uncommon. However, one well-documented additional factor that can increase the depth at which earthquakes can occur is the presence of a pressurized fluid in the pore spaces of the rock (Scholz 1990). Evidence for this phenomenon is found beneath volcanoes, where earthquakes have been detected at depths greater than 50 km, in connection with movement of magma.

0084-6597/95/0515–0169$05.00

Annu. Rev. Earth Planet. Sci. 1995.23:169-213. Downloaded from www.annualreviews.org
by California Institute of Technology on 06/20/13. For personal use only.

However, in addition to these relatively uncommon occurrences, in some regions of the globe abundant earthquakes extend to very great depths, as has been known for over 70 years (Turner 1922, Wadati 1928). In these regions, Wadati-Benioff zones, earthquakes occur along inclined planes that extend down into the Earth's mantle from below ocean trenches to depths approaching 700 km. The modern theory of plate tectonics explains Wadati-Benioff zones as occurring within subduction zones where cold oceanic lithosphere sinks into the mantle as the descending limb of the cold thermal boundary layer of mantle convection. Despite the fact that rocks in subduction zones are much stronger than elsewhere because of their lower temperature, the extreme inhibition of frictional processes imposed by pressure still prevents brittle failure or frictional sliding. For example, even at room temperature, brittle failure of mantle rocks is impossible in the absence of a fluid at pressures above about 3 GPa (equivalent to 100 km depth). Because it is extremely unlikely that a fluid-filled porosity of any significance could be maintained to great depth, it was clear even in the 1920s (e.g. Jeffreys 1929, 1936) that to explain earthquakes deeper than a few tens of kilometers, processes must be sought in the solid lithosphere that are capable of generating a fluid or some other agent to overcome friction. For the purposes of this review, we make the conservative assumption that depth is 70 km along a slab geotherm.

Many different mechanisms for deep earthquakes have been suggested over the years, including plastic instabilities (Bridgman 1936, Orowan 1960, Hobbs & Ord 1988), shear-induced melting (Griggs 1954, 1972; Griggs & Handin 1960; Griggs & Baker 1969), instabilities accompanying recrystallization (Post 1977, Ogawa 1987), and polymorphic phase transformations (Bridgman 1945; Benioff 1963; Evison 1963, 1967; Vaisnys & Pilbeam 1976; Sung & Burns 1976; Liu 1983; Hodder 1984; Kirby 1987; Meade & Jeanloz 1989). The latter category is more highly populated with suggestions than other hypotheses because it was recognized early that the deepest earthquakes occur in the mantle transition zone between abrupt seismic discontinuities that bracket steep seismic velocity gradients. The phase change hypothesis was particularly attractive because the volume reductions involved raised the possibility of a sudden implosion that could radiate seismic energy without faulting, thereby circumventing the friction problem. However, as discussed below, seismic evidence now precludes this possibility because deep earthquakes have double-couple motions similar to those of shallow events.

This review is directed primarily toward delineating the mechanisms by which rocks can fail at high pressure and which aspects of the seismology and petrology of the Earth's mantle support or contradict the operation of those mechanisms. In the following pages we recount in some detail the seismic characteristics of subduction zones and the earthquakes within them, the anatomy of brittle failure, and the discovery and characterization of a fundamentally new

failure mechanism. From these observations we develop a composite model of how earthquakes are generated at intermediate (70–300 km) and great (300–680 km) depths in subducting lithosphere, and why they terminate abruptly at the base of the transition zone. Of course, a true theory of earthquakes must incorporate not only the physics by which the failure occurs, but also a model of the source(s) of the stresses that cause the failure. Although a full discussion of the sources of stress in tectonic slabs is outside the scope of this paper, we do discuss stresses produced by structures inherent in our model. Similarly, in this limited space, it is not our intention to review exhaustively the extensive literature on deep earthquake source properties, slab velocity structure, or brittle/frictional failure, but to set forth the relevant experiments and observations in these broad subjects that enabled the development of a coherent hypothesis of the generation of deep earthquakes. For further details we direct the reader to reviews on source properties of deep earthquakes (Frohlich 1989), seismic structure of subducted slabs (Lay 1994a,b), and brittle failure (Scholz 1989, 1990).

Annu. Rev. Earth Planet. Sci. 1995.23:169-213. Downloaded from www.annualreviews.org
by California Institute of Technology on 06/20/13. For personal use only.

COMPOSITION AND STRUCTURE OF SUBDUCTING LITHOSPHERE

Intermediate and deep earthquakes occur in subducting lithosphere. Because of its creation and long residence time at the Earth's surface, this portion of the mantle is well characterized in terms of its structure and composition. It consists of 5–6 km of basaltic crust overlying 10–15 km of harzburgitic residuum that grades into relatively undepleted lherzolite. Studies of ophiolites and ocean-floor dredge hauls show that the crust is significantly altered by hydrothermal circulation along fractures in the vicinity of oceanic ridges where it is created, and that the immediately underlying mantle is also hydrated (serpentinized) but to a lesser degree. In contrast, mantle xenoliths from oceanic volcanism that sample deeper lithosphere show little or no evidence of hydrous phases, indicating that hydration in bulk falls off rapidly with depth and is probably insignificant below about 10 km. Surface-cutting normal faults generated in the ridge and the trench outer rise environments could have hydrous alteration along them to greater depths, although there is no direct evidence of this.

The progressive deepening of the ocean basins away from ridges varies as the square root of age owing to cooling and thermal contraction. As a consequence the temperature within subducting lithosphere decreases as a function of plate velocity and the age at which it enters the subduction zone (e.g. Stein & Stein 1992). Many complicated processes operate in and around the slab at shallow depths; the most important for the subject under discussion here is the generation of arc volcanism by release of hydrous fluid at ~100 km depth. Progressive warming of the slab takes place by conduction of heat from the overlying mantle wedge, which results in the coldest portion of the slab slowly migrating into its interior (Figure 1).

Annu. Rev. Earth Planet. Sci. 1995.23:169-213. Downloaded from www.annualreviews.org
by California Institute of Technology on 06/20/13. For personal use only.

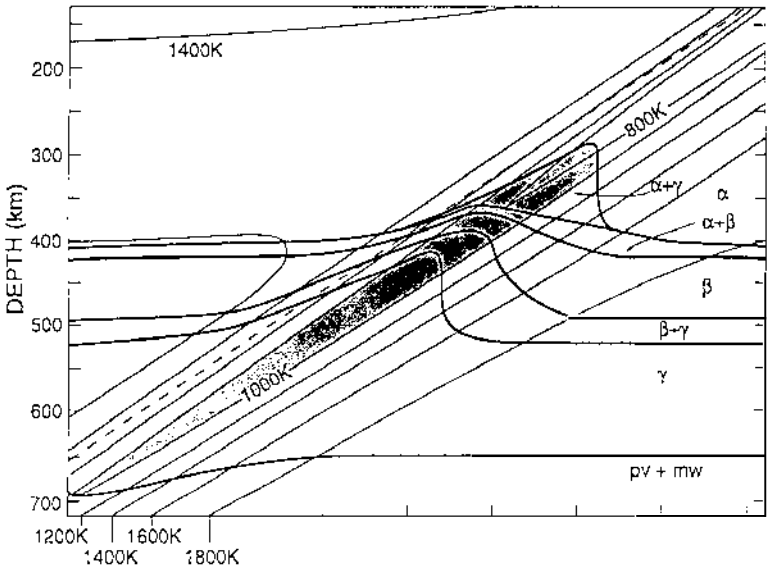

(a)

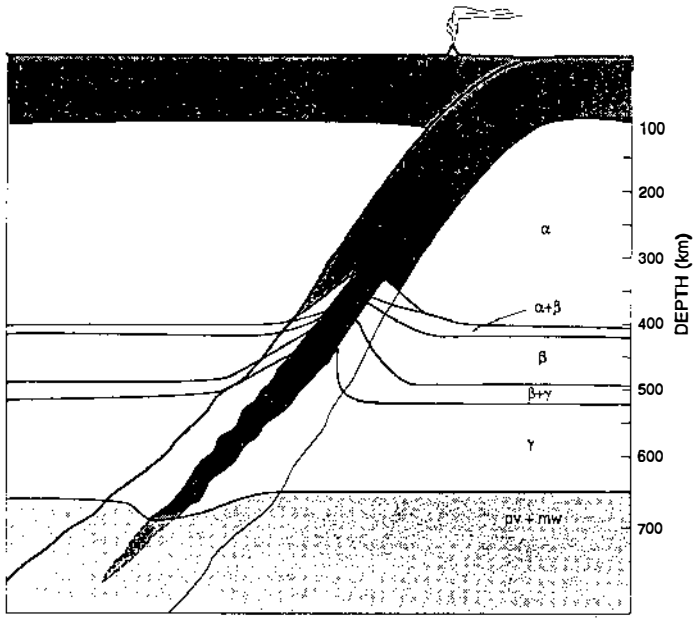

(b)

Annu. Rev. Earth Planet. Sci. 1995.23:169-213. Downloaded from www.annualreviews.org by California Institute of Technology on 06/20/13. For personal use only.

As the lithosphere descends further, it passes through a series of polymorphic phase transformations and mineral reactions. Because of the low temperatures within subducting slabs, the phase transformations of olivine, $(Mg, Fe)_2SiO_4$, to its high-pressure polymorphs is somewhat more complicated than elsewhere (Akaogi et al 1989). Away from slabs, where it is warmer, the transformation to β olivine, which has a spinelloid structure and is about 6% more dense than olivine, takes place at about 410 km and produces the seismic discontinuity that defines the top of the mantle transition zone. However, at lower temperatures, the first appearance of a high-density phase is at much lower pressures and consists of a two-phase field in which Mg-enriched olivine coexists with Fe-enriched γ olivine (Figure 1). The latter has a true spinel structure and is about 2% more dense than β olivine. The β field is reached at greater depth (~370 km in cold slabs); the γ phase reappears along with β at around 400 km and completely replaces β by about 450 km. At about 700 km in slabs, the seismic discontinuity due to disproportionation of the γ phase to $(Mg, Fe)SiO_3$ perovskite plus magnesiowüstite is encountered, with an additional increase in density of about 8%. This latter discontinuity defines the base of the transition zone and is located at about 660 km outside of slabs.

The fate of slabs at the 660 km discontinuity has been a hotly contested issue of recent years, with some proponents arguing for retention of the slab within the upper mantle (implying convective isolation of the upper and lower mantles), others contending that the observations are better modeled with whole-mantle convection, and still others proposing that slabs pause at the 660 km discontinuity but avalanche into the lower mantle periodically (for reviews, see Lay 1994a,b). Convective isolation now appears to be ruled out by seismic tomographic imaging of slabs, which shows that some slabs penetrate the 660 km discontinuity and enter the lower mantle (van der Hilst et al 1991; Fukao et al 1992; Grand 1994; Lay 1994a,b). Other slabs, however, appear slowed or deflected at the boundary, supporting the concept that they encounter significant resistance to entering the lower mantle. Whether this resistance provides a major disruption in convective circulation or a minor one remains an open issue.

Figure 1 (*a*) Thermal model of cold subducting lithosphere showing isotherms (contour interval 200 K) and the phase relations for mantle olivine, $(Mg_{.9}Fe_{.1})_2SiO_4$. Stippled region within the 1000 K isotherm represents a wedge containing metastable olivine that is potentially present due to thermal inhibition of reactions. Greek letters signify olivine (α) and its high-pressure polymorphs (β and γ). [Thermal structure modified after Hellfrich et al (1989), as extended by Kirby et al (1991); phase boundaries from Akaogi et al (1989).] (*b*) Cartoon incorporating slab deformation. The ubiquitous slab-parallel compression indicated by deep earthquake source mechanisms implies thickening of the metastable wedge and contributes to its preservation to great depth. Dark stippling—olivine-bearing lithosphere; light stippling—lower mantle. Any olivine surviving into the lower mantle (*dashed line* outlining *intermediate stippling*) would decay aseismically to perovskite + magnesiowüstite.

Annu. Rev. Earth Planet. Sci. 1995.23:169-213. Downloaded from www.annualreviews.org
by California Institute of Technology on 06/20/13. For personal use only.

SEISMIC CHARACTERISTICS OF INTERMEDIATE AND DEEP EARTHQUAKES

Most seismological properties of intermediate (70–300 km) and deep (300–680 km) earthquakes are grossly similar to those of shallow earthquakes. Probably the most conspicuous difference between deep and shallow earthquakes is the rate of production of aftershocks. The incidence of aftershocks is considerably less common for events deeper than 70 km than for shallower events. Below 450 km there is a moderate increase in the incidence of aftershocks compared to events from 70 to 450 km (Frohlich 1987).

Earthquake Depth and Size Distribution

The frequency of earthquakes in subduction zones decreases exponentially with depth down to about 300 km, then increases again between 400 and 600 km before dropping off abruptly between 600 and 680 km (Figure 2) (Frohlich 1989). This general pattern, of a minimum in seismicity separating intermediate and deep earthquakes, is observed in all subduction zones with deep seismicity, although the depth of the minimum varies slightly from zone to zone (Helffrich & Brodholt 1991). Its shallowest occurrence is in the Izu-Bonin subduction

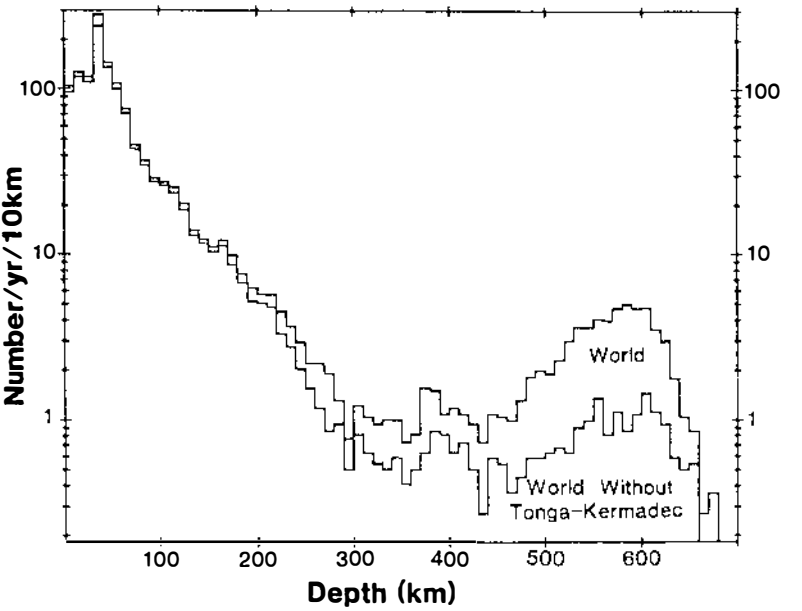

Figure 2 Number of earthquakes per year from 1/64 to 2/86 having $m_b \geq 5.0$. Upper curve is all earthquakes; lower curve has had those from Tonga-Kermadec removed to show that the two populations are not restricted to Tonga. (From Frohlich 1989.)

zone, where the seismicity minimum lies between 250 and 350 km, and the deep seismicity occurs between 350 and 550 km.

Earthquakes deeper than 70 km generally follow a distribution with size similar to shallower ones. Their numbers decrease exponentially with increasing size, according to the Gutenberg-Richter magnitude-frequency relation: $\log[n(M)] = A - bM$, where n is the number of earthquakes with magnitude greater than M, A is a constant that measures the level of seismic activity, and b is a constant that describes the size distribution. b-values of about 1.0 are typical for both shallow and deep earthquakes. However, particular subduction zones exhibit anomalous b-values for deep earthquakes. A b-value of 1.2 was found for Tonga, whereas that in South America was 0.4 (Giardini 1988, Frohlich 1989). Thus, compared to the average distribution, deep seismicity in Tonga is biased toward small events, whereas in South America it is biased toward large events (vividly demonstrated by the great Bolivian earthquake of June 9, 1994, which occurred during preparation of this manuscript).

There is a remarkable tendency for the largest deep earthquakes to occur on the margins of the Wadati-Benioff zone, sometimes separated from other seismicity by hundreds of kilometers. This is demonstrated by the locations of the five largest deep earthquakes recorded in modern times: beneath Bolivia on June 9, 1994 (650 km, 3×10^{28} dyn-cm); Colombia on July 31, 1970 (650 km, 2×10^{28} dyn-cm); Peru-Bolivia on August 15, 1963 (600 km, 7×10^{27} dyn-cm); Spain on March 29, 1954 (630 km, 7×10^{27} dyn-cm); and Tonga on March 9, 1994 (575 km, 3×10^{27} dyn-cm). (The 1994 Bolivian event is the largest event, deep or shallow, to occur since the 1977 shallow normal faulting Sumba). The first four events occurred in regions with anomalously low levels of smaller seismicity. Furthermore, a tendency has been noted for the larger events in several subduction zones to occur near the margins of the seismically active portions of the zone. This phenomenon has been noted in Izu-Bonin, Japan, the Kuriles (K Creager, personal communication), and Java (Okal et al 1993).

Source Geometry

The geometry of seismic motion is generally described by a symmetric second-rank tensor called the *seismic moment tensor,* which can be expressed as the sum of three tensors representing double-couple (slip on a single fault plane), isotropic (explosive or implosive), and compensated linear vector dipole (CLVD, volume-preserving, axially symmetric) components, respectively. Deep earthquakes are similar to shallow earthquakes in that they are primarily the result of double-couple motions. Although an isotropic implosive component for deep earthquakes has long been sought as a manifestation of the volumetric change associated with phase transformations in the downgoing slab, unambiguous detection has proved elusive (Frohlich 1989). The sig-

Annu. Rev. Earth Planet. Sci. 1995.23:169-213. Downloaded from www.annualreviews.org by California Institute of Technology on 06/20/13. For personal use only.

nificant isotropic components for the 1970 Colombia and 1963 Peru-Bolivia earthquakes found by Gilbert & Dziewonski (1975) remain controversial (e.g. Okal & Geller 1979). Kawakatsu (1991) analyzed the long-period body-wave trains for 19 recent, large, deep earthquakes and determined that they all had isotropic components of less than 10%, which is close to the resolution of the method. For the two largest deep earthquakes of the past 24 years, both of which occurred in 1994 and were consequently well-recorded, the amount of isotropic component observed was insignificant (G Ekstrom, personal communication).

In contrast, the CLVD component of deep earthquakes is significant in many cases. The average amount of CLVD is greater for intermediate and deep earthquakes than for shallow ones (Kuge & Kawakatsu 1993). Some well-recorded, large, deep earthquakes have quite large and clearly resolved CLVD components. In this regard, the behavior of the largest deep earthquakes is mixed: The 1970 Colombia and 1963 Peru-Bolivia earthquakes possess quite large CLVD components (Gilbert & Dziewonski 1975, Okal & Geller 1979), but the 1994 Tonga and 1994 Bolivia earthquakes have insignificant CLVD [according to the Harvard CMT (centroid moment tensor) catalog]. Analysis of broadband body waves of several deep earthquakes with a well-resolved large CLVD component suggests that they may result from almost simultaneous movement on two nonparallel planes in which the slip direction of at least one of the faults is oblique to their line of intersection (Kuge & Kawakatsu 1993). This is currently the preferred explanation for the CLVD component.

Stress Release

Determining the magnitude of stress release in deep earthquakes has been the focus of many studies (e.g. Mikumo 1971, Wyss & Molnar 1972, Chung & Kanamori 1980, Abe 1982, Fukao & Kikuchi 1987; for a review, see Frohlich 1989). These efforts seek to identify the variations in stress drops with depth that might be expected to accompany the great changes in pressure from the surface to 700 km depth. Until recently, the behavior of stress drop with depth has been unclear due to the small numbers of events studied, coupled with the intrinsic large scatter in this quantity. Houston & Williams (1991) computed stress drops of 68 deep and intermediate earthquakes using source spectra obtained from digital broadband body waveforms. Seismically radiated energy was calculated from the squared velocity source spectra, and employed in the computation of stress drops using the ratio of energy to moment. The stress drops average about 2 MPa, show no trend with depth, and are similar to those of earthquakes occurring in the outer rise of ocean plates before they subduct (Figure 3*a*). These results are generally consistent with those of previous studies taken together, considering that the extensive literature on stress drops shows them to vary intrinsically by an order of magnitude in addition to their substantial sensitivity

Annu. Rev. Earth Planet. Sci. 1995.23:169-213. Downloaded from www.annualreviews.org
by California Institute of Technology on 06/20/13. For personal use only.

Annu. Rev. Earth Planet. Sci. 1995.23:169-213. Downloaded from www.annualreviews.org
by California Institute of Technology on 06/20/13. For personal use only.

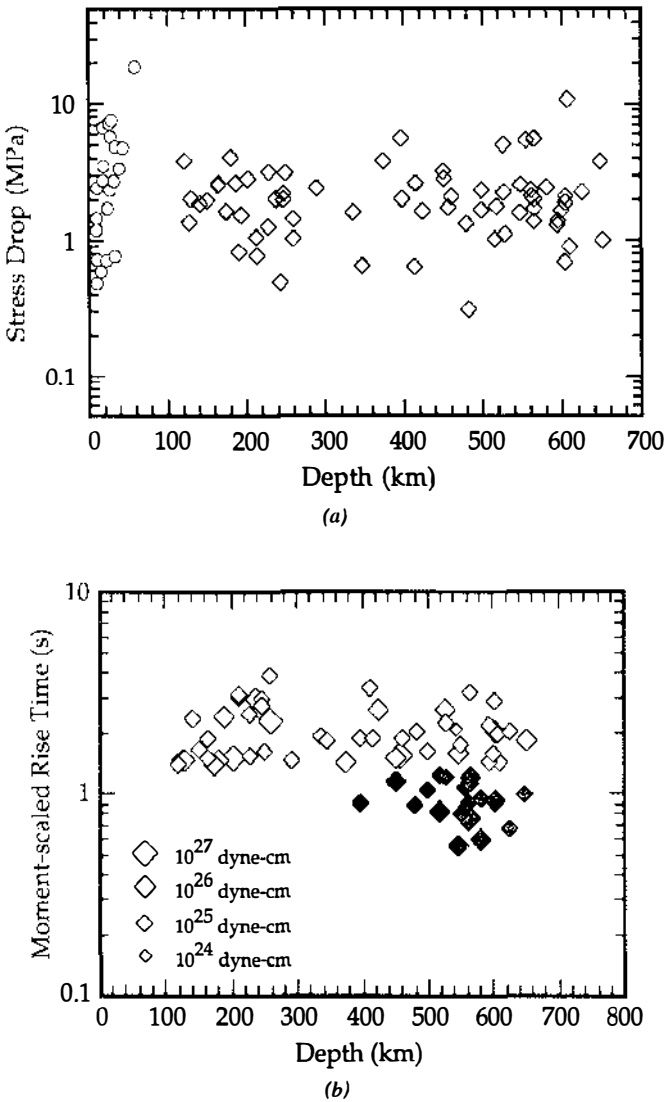

Figure 3 (*a*) Stress drop vs earthquake depth. Stress drops computed using the energy:moment ratio (equivalent to twice the apparent stress) show no trend with depth. Intermediate and deep events (*diamonds*) from Houston & Williams (1991). Open circles represent outer rise earthquakes in the oceanic lithosphere. (*b*) Rise times (the time from the onset of faulting to the peak moment release rate) vs earthquake depth. The fastest rise times are for earthquakes below 450 km depth. The rise times have been scaled by the cube root of the seismic moment (normalized by 10^{26} dyn-cm) to remove the effect of earthquake size. (After Houston & Williams 1991.)

to the measurement technique. Thus, the stress released in deep or intermediate earthquakes does not differ significantly from that in shallow earthquakes in a comparable tectonic setting, i.e. within, as opposed to between, tectonic plates. Interplate earthquakes, however, have on average somewhat smaller stress drops than intraplate events (Kanamori & Allen 1986).

Temporal Source Properties

Annu. Rev. Earth Planet. Sci. 1995.23:169-213. Downloaded from www.annualreviews.org by California Institute of Technology on 06/20/13. For personal use only.

In contrast to the similarities noted above in size distribution, double-couple nature, and stress release, several recent studies reveal differences in temporal aspects of rupture processes for deep and intermediate earthquakes. Houston & Williams (1991) measured the time from the onset of slip until the peak moment release rate was recorded at broadband, teleseismic stations for 68 intermediate and deep earthquakes. These rise times, when scaled for earthquake size, showed a decrease of almost a factor of two in their average, as well as an increase in variability, below 450 km depth (Figure 3*b*). This change can be interpreted as an increase in rupture velocity or particle velocity across the fault; unfortunately without very dense station coverage, it is rarely possible to distinguish between these two possibilities using seismic data.

Although the duration of rupture is a fundamental characteristic of earthquakes, the complexity and incoherence of the seismic source at high frequencies often inhibit the identification of features in the later part of rupture, complicating the measurement of rupture durations. Vidale & Houston (1993) measured durations of 122 intermediate and deep earthquakes from stacks of hundreds of teleseismic records from regional arrays. Stacking produces an unusually clear depiction of the earthquake source at short periods by cancelling background noise and reverberations generated near the receivers. The ending, as well as the beginning, of rupture is clearly identifiable for most intermediate and deep earthquakes studied and is often surprisingly abrupt. Vidale & Houston found a decrease in the duration of about a factor of two from 100 to 600 km depth (Figure 4). Simple models of faulting suggest that duration should be inversely proportional to the shear wave velocity and to the cube root of stress drop. Thus, to explain the observed twofold decrease in duration with depth, stress drops would have to increase by a factor of four, as shear velocity increases with depth by only about 20%. However, as discussed above, observed stress drops show no strong trend with depth (Houston & Williams 1991), which indicates that some aspect of the rupture process must change with depth. To constrain the type of changes that may occur, Houston & Vidale (1994) compared the shape of the envelope of seismic radiation for deep and intermediate events, again using the stacks of regional array records. On average, for intermediate depth events, more radiation is released toward the beginning of the rupture than near the end; for deep events radiation is released symmetrically over the duration of the event, and is marked by an abrupt beginning and

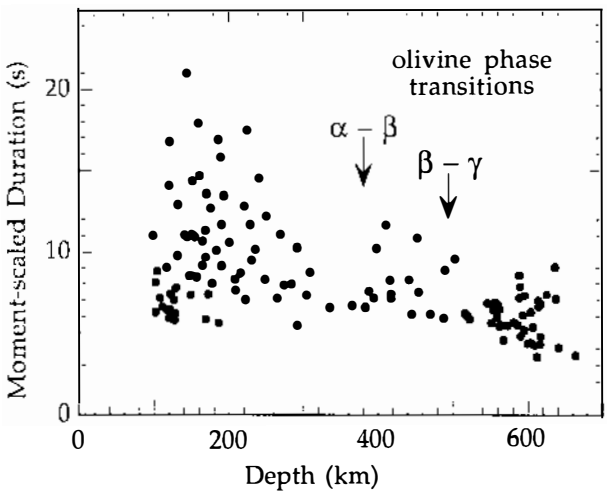

Figure 4 Rupture duration vs earthquake depth. The durations have been scaled by the cube root of the seismic moment to remove the effect of earthquake size. The durations decrease with depth from 100 to 600 km depth by about a factor of two, which is greater than that expected from source scaling relations, suggesting a change in the style of rupture with depth. The depths of the equilibrium phase transitions of olivine in cold subducting slabs are shown. (After Vidale & Houston 1993.)

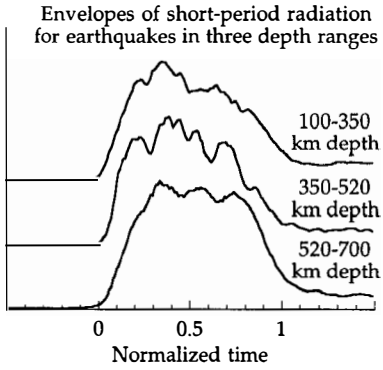

Figure 5 Average envelopes of stacked waveforms of events grouped by depth ranges 100–350 km, 350–520 km, and 520–700 km. The average envelope in the 100–350 km depth range is asymmetric, ending more slowly than it begins; at greater depths the envelope is more symmetric. (After Houston & Vidale 1994.)

end of rupture (Figure 5). This change in envelope shape suggests a variation in the style of rupture related to decreasing fault heterogeneity with increasing depth (Figure 6).

Stress Orientations

The orientation of stress release in Wadati-Benioff zones has been studied extensively with earthquake focal mechanisms. The compressional axes of

Annu. Rev. Earth Planet. Sci. 1995.23:169-213. Downloaded from www.annualreviews.org
by California Institute of Technology on 06/20/13. For personal use only.

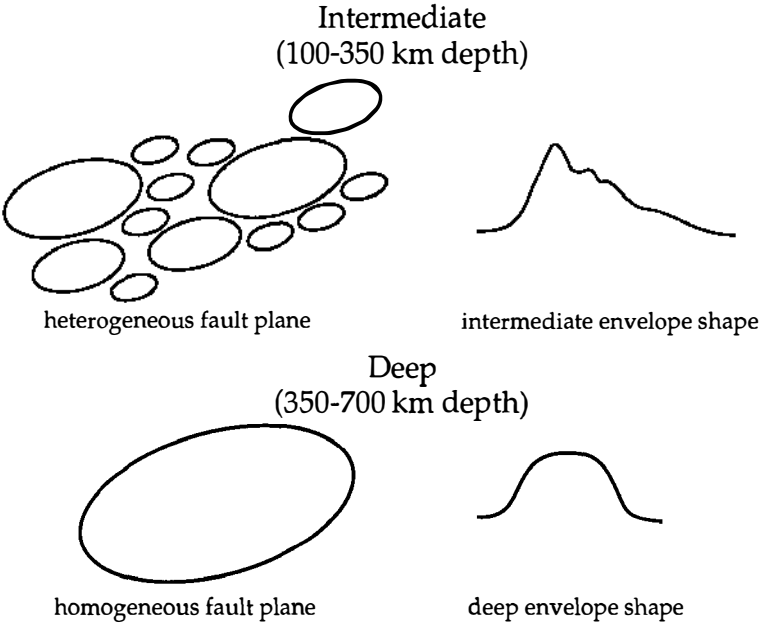

Figure 6 Schematic illustration of the possible role of fault heterogeneity in envelope shape and rupture duration. Greater heterogeneity at intermediate depths may result in a relatively long duration and asymmetric envelope, whereas greater homogeneity deeper may result in a shorter duration and more symmetric envelope. (After Houston & Vidale 1994.)

earthquakes deeper than 400 km align consistently in the down-dip direction of the slab (Isacks & Molnar 1971, Apperson & Frohlich 1987). The stress at intermediate depths is more variable, partly because there are more subduction zones with intermediate-depth seismicity than with deep seismicity. However, the earlier studies found that for intermediate-depth earthquakes in subduction zones lacking deep seismicity, the stress was almost invariably down-dip tensional, and that this pattern was also obtained for some slabs with deep seismicity. In the latter subduction zones, the intermediate-depth, tensional, solutions were separated from the deeper, compressional, ones by a distinct minimum in seismic activity. The interpretation of these systematics was that for most subduction zones intermediate depths were under tension due to the negative buoyancy of the cold slab, and that deep portions of slabs were under compression because they encountered increased resistance near the base of the transition zone (Richter 1979, Vassiliou et al 1984). The existence of the seismicity minimum between these two regimes allowed a convenient interpretation as a zone of low stress where the regional stress field went through zero around 300 km. Earthquakes were considered to stop when the temperature reached the point at which failure was no longer possible.

Annu. Rev. Earth Planet. Sci. 1995.23:169-213. Downloaded from www.annualreviews.org
by California Institute of Technology on 06/20/13. For personal use only.

Annu. Rev. Earth Planet. Sci. 1995.23:169-213. Downloaded from www.annualreviews.org by California Institute of Technology on 06/20/13. For personal use only.

It is becoming increasingly clear, however, that the data do not support this simple thermo-mechanical model. Recent global analyses of stress orientations incorporating thousands of focal mechanisms from the Harvard CMT catalog demonstrate that in many zones possessing deep seismicity the intermediate-depth seismicity (still separated from the deep seismicity by a distinct minimum) also is often in a state of down-dip compression (Zhou 1990, Houston & Zhang 1992, Lundgren & Giardini 1992). Such zones include Tonga, Solomon Islands, Japan, Izu-Bonin (Figure 7*a*), the Philippines, and much of the Kuriles (Figure 7*b*). There is also some evidence for down-dip compression at intermediate depths above that portion of the Java slab that possesses deep seismicity. The main exceptions are the Marianas and South America, for which the intermediate-depth seismicity is down-dip tensional. Thus, the majority of slabs with deep seismicity show down-dip compressional solutions above the seismicity minimum; consequently, the minimum is difficult to understand in the context of the thermo-mechanical model. Moreover, it is difficult to retain the argument that the slab serves as a stress guide when it must transmit resistance at depth through the minimum to generate down-dip compression above. Furthermore, most slabs, including those that are seismically active only down to intermediate depths, have been subducting sufficiently rapidly and for long enough times that they are expected to extend at least to the base of the upper mantle. Based on our current understanding of slab rheology, even these relatively young, slow (hence warmer) slabs appear to be mechanically strong down to the base of the upper mantle (Brodholt & Stein 1988). Thus, like slabs displaying deep seismicity, these young, slow slabs also would be expected to transmit compressive stress to intermediate depths if the origin of that stress is resistance to slab penetration. In the absence of a coherent explanation of the observed stresses consistent with what is known about slab rheology, these systematics seem to require that deep and intermediate earthquakes are generated by two different failure mechanisms operating in different depth ranges.

Internal Structure of Deep Subduction Zones

If subducting slabs are sufficiently cold to kinetically inhibit the polymorphic transformations that should occur in olivine (discussed at length below), a wedge of metastable olivine would exist in at least the coldest slabs and could be involved in the generation of deep earthquakes. Such a metastable wedge would be associated with a low-velocity anomaly of about 5% in the core of the slab (Vidale et al 1991). Efforts to detect such a body seismically are based on the effects of the wedge on travel times or on waveforms, which would be distorted by such a structure. Recent seismic measurements of the depth of the olivine to β-phase transformation that occurs near 410 km outside subduction zones show 10 to 30 km of elevation adjacent to subduction zones (Vidale & Benz 1992). This elevation of the transformation implies temperatures about

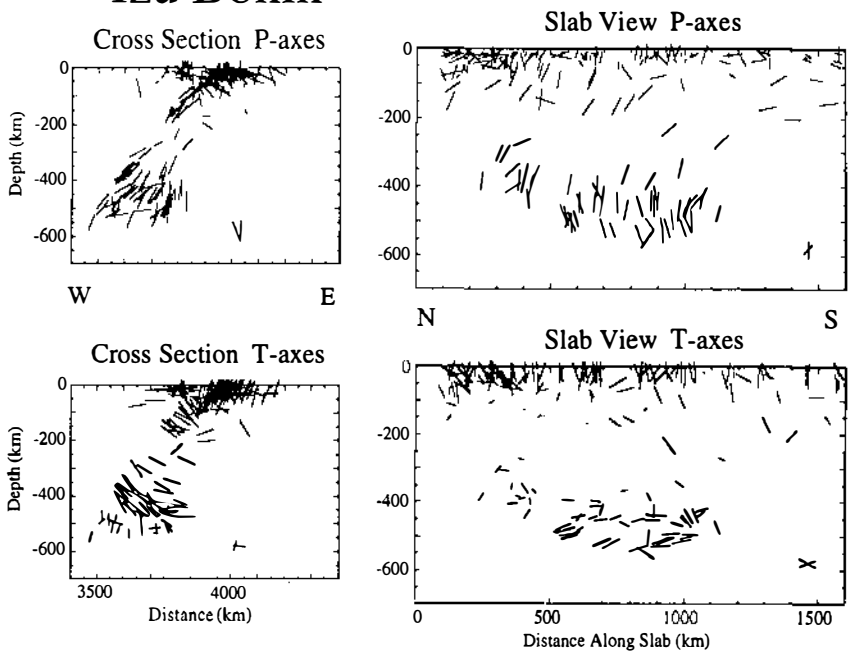

(a)

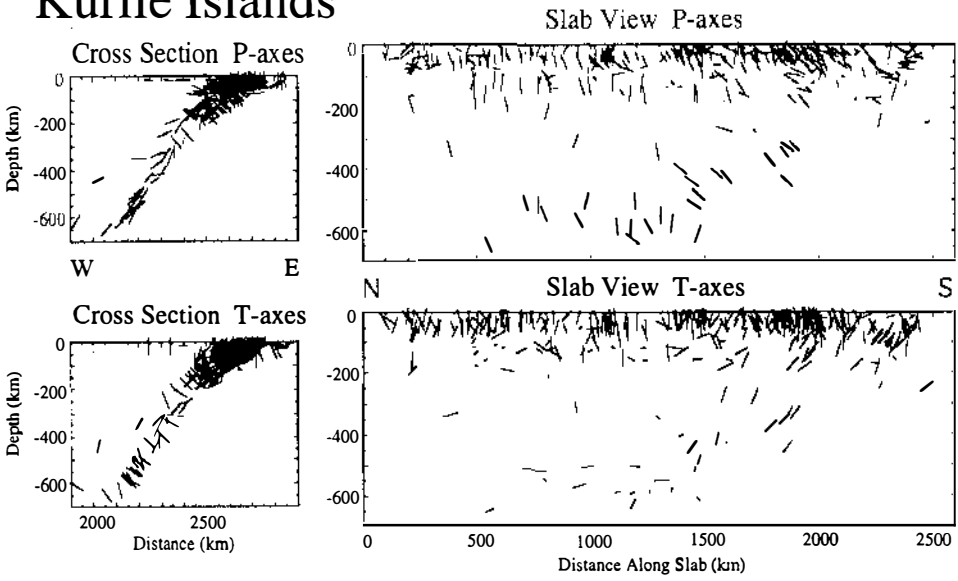

(b)

Annu. Rev. Earth Planet. Sci. 1995.23:169-213. Downloaded from www.annualreviews.org
by California Institute of Technology on 06/20/13. For personal use only.

Annu. Rev. Earth Planet. Sci. 1995.23:169-213. Downloaded from www.annualreviews.org
by California Institute of Technology on 06/20/13. For personal use only.

800 K less than in ambient mantle—consistent with our thermal understanding of slab thermal structure (Figure 1*a*). These results still allow the presence of a metastable wedge in the core of the slab because the seismic waves utilized tend to sample the flanks rather than its central coldest portion.

Iidaka & Suetsugu (1992) compared travel times observed in Japan traveling up-dip along the northern Izu-Bonin slab to predictions from velocity models with and without a low-velocity metastable wedge. The observed travel times were much better fit by the metastable model. However, the locations of the phase boundaries in the slab models compared by Iidaka & Suetsugu (1992) were taken from older models in the literature that had been constructed without benefit of current knowledge of the olivine phase diagram or modern thermal models of slabs. The equilibrium model they used postulated that the $\alpha \rightarrow \beta$ olivine phase boundary, which defines the top of the transition zone distant from slabs, is elevated within the slab by 130 km. Thus, they assumed that the denser polymorphs of olivine occupy the entire slab below the phase boundary, and they assigned to that region the appropriate higher seismic velocity. However, as pointed out above, under slab conditions, currently accepted phase relations for olivine of mantle composition (Akaogi et al 1989) show that the first densification reaction encountered under subduction zone conditions is $\alpha \rightarrow \alpha + \gamma$ (Figure 1). Thus, under equilibrium conditions, at depths of ~290–370 km in a cold slab (e.g. Helffrich et al 1989) a two-phase assemblage exists, which reacts at ~370 km to form β olivine. The pressure-temperature (P-T) conditions for the $\alpha + \gamma$ field at the low temperatures found in subducting slabs were derived by Akaogi et al (1989), who extrapolated the experimental relations of Katsura & Ito (1989); hence, the exact ratio of α to γ along the geotherm from 290 to 370 km is somewhat uncertain. We assume that the topology of the phase

Figure 7 (*a*) Stress orientations (P = maximum compression; T = maximum extension) from the Harvard CMT catalog for all events near Izu-Bonin (23° < latitude < 35° and 136° < longitude < 144°). P and T axes are shown in two curvilinear projections: a trench-normal projection, onto a vertical plane between each event and a specified pole (22°, 103°), and an along-slab-strike projection onto a portion of a cylinder of radius 35° whose axis intercepts the pole and dips 55°. The shorter the axis the greater its angle to the plane of projection. The predominant seismic strain below 100 km depth in the slab is down-dip compressional. The southern end of the slab view is part of the Marianas subduction zone, where the intermediate depth strains are complex and may be related to the tight curvature of that zone. (*b*) Stress orientations from the Harvard CMT catalog for all events in the Kuriles (42° < latitude < 60° and 139° < longitude < 164°). P and T axes are shown in two curvilinear projections: a trench-normal projection, onto a vertical plane between each event and a specified pole (61°, 120°), and an along-slab-strike projection onto a portion of a cylinder of radius 23° whose axis intercepts the pole and dips 50°. The shorter the axis, the greater its angle to the plane of projection. The predominant seismic strain below 100 km depth in the slab is down-dip compressional. The strain in the southern part of the arc may be related to the shallowing of the slab near the Hokkaido corner. (From Houston & Zhang 1992.)

diagram remains the same as at higher temperatures (Figure 8 of Akaogi et al 1989), and derive that, within the two-phase region, the fraction of γ goes from zero at 290 km to about 50% at 370 km.

The relations in the preceding paragraph show that the travel-time residuals calculated by Iidaka & Suetsugu (1992) for the equilibrium case are too high. Based on the fractions of the phases in this region, we have reestimated the difference in travel-time residuals for the two models. We assumed that Iidaka & Suetsugu's calculations appropriately characterize the difference between the two models along the cold core of the slab from the earthquake source to 370 km (0.4 km s^{-1}) and that the velocity in the two-phase region varies from 0.2 km s^{-1} greater than that for olivine to zero difference. From these values, we estimate that the difference in travel-time residuals for the two models for earthquakes in the depth range 300–350 km should be reduced by about 90% (~0.25 sec); for earthquakes at greater depths the overestimation of residuals should be ~0.3 sec. Subtracting these values from the differences shown in their Figure 3 leaves differences between the models of essentially zero for 300–350 km, 0.3 sec for 350–400 km, 0.6 sec for 400–450 km, and 0.9 sec for 450–500 km.

Although these corrections reduce the differences between the two models of Iidaka & Suetsugu (1992), a significant difference remains for earthquakes in the 400–450 km depth range, and for the greatest depth range (450–500 km) the equilibrium model still falls outside their error bars. Given the dense coverage of seismic stations directly above the slab in Japan and consequent detailed knowledge of the seismic velocity structure there, this remains a robust result. Furthermore, as described below, laboratory kinetic data support the presence of a metastable olivine wedge for all old, rapidly subducting, slabs.

Detection of a low-velocity wedge in slabs using waveforms has proved more difficult for the reasons outlined in Vidale et al (1991). These include complexity in the earthquake source time-function, a lack of seismicity at the optimum depth (near 400 km for downgoing teleseismic waves), a strong dependence of waveform distortion on the source location in the direction perpendicular to the slab, and a lack of sufficiently dense broadband station coverage. Nevertheless, these limitations will probably be overcome as improved data become available.

The location of the Wadati-Benioff zone within the slab is important for understanding the failure mechanism. The switch from underthrusting focal mechanisms at shallow depths to one of the principal stresses down-dip at intermediate depths is generally interpreted as evidence of migration of the earthquakes into the interior of the slab. One firm piece of evidence for earthquakes moderately deep into the slab is the existence of double seismic zones. Such zones have been detected at shallow to intermediate depths (e.g. in Japan, Hasegawa et al 1978; in Tonga, Kawakatsu 1986; in the Aleutians, Abers 1992; in the Kuriles, Kao & Chen 1994), and recently also at depths in excess of

Annu. Rev. Earth Planet. Sci. 1995.23:169-213. Downloaded from www.annualreviews.org
by California Institute of Technology on 06/20/13. For personal use only.

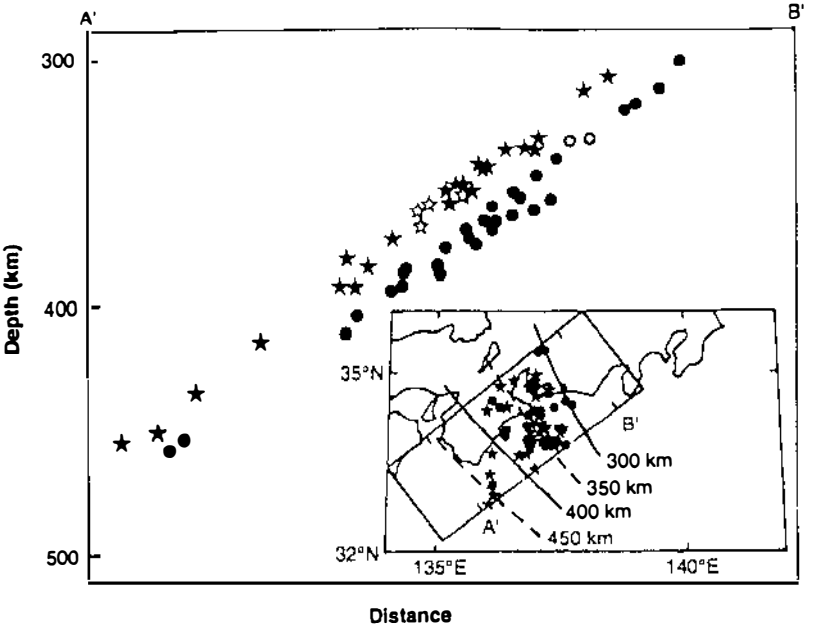

Figure 8 Hypocenters of earthquakes defining a deep double seismic zone in Izu-Bonin subduction zone. Open symbols show converted phases that allow delineation of the upper boundary of the slab 15–20 km above upper zone. Insert shows a map of epicenters with lines of constant depth. (From Iidaka & Furukawa 1994.)

300 km (in Tonga, Wiens et al 1993, and in Izu-Bonin, Iidaka & Furukawa 1994). The latter double zone (Figure 8) is from the same area where Iidaka & Suetsugu (1992) reported evidence of a metastable olivine wedge. In all but one double zone for which focal mechanisms were determined, one of the two zones showed down-dip compression and the other down-dip tension; this configuration can be interpreted in terms of slab-bending stresses. The spacing between the zones is typically 25–40 km, implying that earthquakes can occur at least this far below the top of the slab. Additional direct evidence of earthquake location within the slab comes from phase conversion of seismic waves at the top of the slab due to the high-velocity crust that has been converted to eclogite (Matsuzawa et al 1990, Hasegawa et al 1991, Iidaka & Furukawa 1994, Zhao & Sacks 1994). Thus, intermediate and deep seismicity occurs within subducting lithosphere up to 40 km below the slab surface.

In summary, intermediate and deep earthquakes occur within the subducting lithosphere, in lithologies dominated by olivine or its high-pressure polymorphs. The depth-dependence of earthquake frequency shows a bimodal distribution, providing a natural division at a depth of 300 km into intermediate and deep events. Many of the source properties of deep earthquakes are similar to those

Annu. Rev. Earth Planet. Sci. 1995.23:169-213. Downloaded from www.annualreviews.org
by California Institute of Technology on 06/20/13. For personal use only.

of intermediate and shallow ones, but subtle differences do exist. Moreover, the systematics of stress orientations and earthquake depth distribution are difficult to reconcile with stresses produced from the negative buoyancy of the cold slab together with resistive viscous forces. Another observation currently lacking explanation is that in the deepest Wadati-Benioff zones, earthquakes terminate at the base of the upper mantle, despite the fact that in at least three cases seismic tomography indicates that slabs enter the lower mantle. Furthermore, deep double seismic zones have been detected in two slabs, with evidence for the existence of a low-velocity metastable wedge reported from one of them. The sum of these observations and the likely disappearance of hydrous phases by about 300 km (discussed below) strongly suggest the operation of two different failure mechanisms, which act in different depth ranges (first suggested by Sykes 1966).

Annu. Rev. Earth Planet. Sci. 1995.23:169-213. Downloaded from www.annualreviews.org
by California Institute of Technology on 06/20/13. For personal use only.

DEHYDRATION-INDUCED BRITTLE FAILURE

In the introduction we summarized why earthquakes deeper than 70 km require the presence of a fluid but pointed out that maintenance of a pore fluid to very great depths is unlikely. However, at least the uppermost several kilometers of lithosphere experience hydrous alteration between the time the lithosphere is generated at an ocean ridge and the time it is subducted, suggesting that one possibility for producing high-pressure faulting involves the generation of a pore fluid by dehydration of hydrous minerals. Experimental deformation of serpentinite above 800 K at a confining pressure of 0.3 GPa by Raleigh & Paterson (1965) showed that this mechanism is indeed viable. Moreover, Meade & Jeanloz (1991) detected acoustic emissions during dehydration of serpentinite in diamond-cell experiments for pressures up to 9 GPa, suggesting that the dehydration embrittlement mechanism can operate at any pressure, given a suitable source of fluid. Thus, if a source of volatiles is available, this mechanism could, in principle, explain earthquakes at any depth. The critical questions, then, are 1. Is it likely that there is a sufficient source of volatiles in the interior of subducting lithosphere? and 2. Is the distribution of intermediate and deep earthquakes in space and time consistent with this mechanism? We conclude below that for intermediate-focus earthquakes the answer is a qualified yes to both questions, but that for deep earthquakes the answers are probably no.

To evaluate whether this mechanism is a likely candidate for producing earthquakes, we need to understand the underlying physics of the failure process in detail. Traditionally, pore-pressure-induced faulting has been attributed in a loose way to partial support of the normal stress across the fault by the fluid, which causes the fault to behave as if the rock were at lower pressure and enables the shear stress to overcome friction. In detail, however, this is not a clear picture. Consider a preexisting fault. It is incorrect to imagine the physical presence of the fluid all along the fault because experimental evidence shows that the fluid does not affect the coefficient of friction on the fault and that the fluid pres-

sure that induces faulting is less than the normal stress on the fault. For either of these to be true, the fluid cannot physically be there as a film on the fault surface; it must be confined to the pore space of the rock. Indeed, the pore pressure must be less than the least principal stress or it would induce tensile failure (hydrofracturing) rather than faulting. The physical role of the pore fluid becomes even more murky when one thinks about generation of a new fault, because then one is appealing to the pore fluid to partially prop open a fault that doesn't exist yet.

The resolution of this conundrum lies in the details of the failure mechanism (Figure 9). In brittle failure, as one raises the stress, the tensile strength is reached locally at stress-concentrating inhomogeneities and tensile microcracks are generated. Such a crack propagates away from the stress riser, curves progressively as the crack tip strives to maintain the lowest energy orientation in the stress field (perpendicular to the local least principal stress), and stops when the stress at the crack tip falls below the tensile strength. These cracks are defined as Mode I features in the fracture mechanics literature because the displacements across them are perpendicular to the plane of the feature. As the macroscopic stress continues to rise, the tensile strength is exceeded locally at an increasing rate. If one monitors the specimen with piezoelectric transducers, a steadily increasing rate of acoustic emissions is found as cracking events associated with these local tensile failures are recorded; as the stress approaches the macroscopic compressive strength, the acoustic emission rate increases exponentially. Finally, in some local region(s), the specimen becomes so fractured that it loses its ability to support the compressive load. At that time, in response to the rearrangement of stresses around the failed region, a self-organization of the tensile fracturing takes place such that a small disk of fault forms at an angle of about 30° to the compression axis (Lockner et al 1991, 1992). The perimeter of the fault disk is bounded by a narrow ring of damaged material called the *process zone,* which is populated by a high density of tensile microcracks, confirming a model put forth by Petit & Barquin (1988) from postmortem examination of faulted specimens. Unless specific countermeasures are taken, once nucleated the fault grows catastrophically and failure occurs on a very short time scale as the elastic energy stored in the loading apparatus is converted to kinetic energy. In a series of spectacular experiments, Lockner et al (1991, 1992) showed that fault growth could be controlled by servoing the computer off of the acoustic emission rate. Fault growth occurred by steady outward migration of the process zone in the plane of the fault, much like expansion of a dislocation loop in a crystallographic glide plane (Green 1992). Indeed, the process zone *is* a dislocation in the sense that it is the boundary between slipped and unslipped regions. If the analogy to crystal dislocations were complete, all shearing action would occur in the process zone, with no bulk sliding on the fault at all. Lockner et al's results showed that at least to a first approximation, this was true; three-dimensional location of the sites of

Annu. Rev. Earth Planet. Sci. 1995.23:169-213. Downloaded from www.annualreviews.org by California Institute of Technology on 06/20/13. For personal use only.

Annu. Rev. Earth Planet. Sci. 1995.23:169-213. Downloaded from www.annualreviews.org
by California Institute of Technology on 06/20/13. For personal use only.

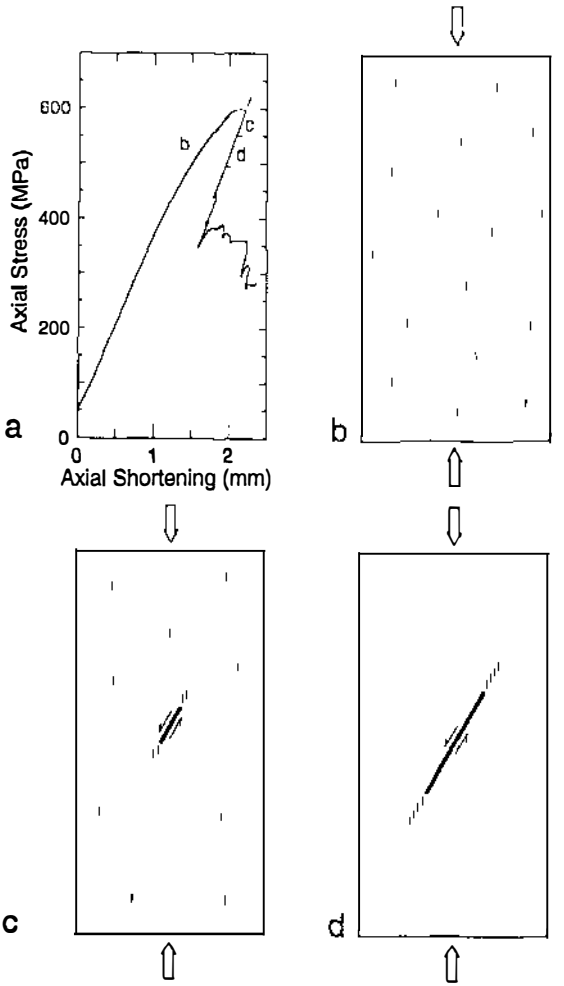

Figure 9 Process of brittle failure. (*a*) Stress-displacement curve for specimen of Westerly Granite compressed at a confining pressure of 50 MPa; letters signify crack distribution schematically presented in similarly labeled panels (from Lockner et al 1991). (*b*) Microcrack distribution during loading. (*c*) Initiation of failure—embryonic fault surrounded by process zone. (*d*) Fault propagation led by process zone of tensile microcracks.

acoustic emissions during growth of the fault showed that almost all of the emissions originated in the process zone.

These experiments document two very important points. First, they demonstrate that brittle failure is fundamentally a tensile process, whether it occurs in macroscopically tensile or compressive mode; in the former, failure results from runaway of a single tensile crack, whereas in the latter, failure is the result

Annu. Rev. Earth Planet. Sci. 1995.23:169-213. Downloaded from www.annualreviews.org
by California Institute of Technology on 06/20/13. For personal use only.

of self-organization of myriads of tensile microfractures into a fault oblique to the principal stress axes. Second, the accurate image of the failure process afforded by these experiments allows insight into how and why pressure severely inhibits it and how pore pressure overcomes that inhibition. Because brittle failure is fundamentally a tensile process, the work of dilation must be performed against the ambient pressure. Thus, opening of Mode I microcracks must occur during loading or the instability will not be triggered. In addition, the Mode I cracks of the process zone must open during fault growth or the instability will be quenched. It is clear, therefore, that a pore fluid operates in concert with the deviatoric stress in the opening of microcracks by filling them as they form at a pressure such that the deviatoric stress can provide the remaining work to create them. This understanding of the process also explains why a pore pressure doesn't reduce the coefficient of friction on the fault. The coefficient of friction is a measure of the entire complicated process of dilation and sliding on a surface. Because the process is the same with or without the pore pressure, the coefficient does not change. In the case of dehydration embrittlement, the fluid may actually be generated locally as part of the local failure process; this would explain why it is available to the growing fault even when the fault is growing at the shear wave velocity. If the hydrous phase is present all along the path and is ripe for dehydration, the necessary pore pressure could be generated in situ as the process zone arrives in advance of the fault or the new slip pulse on a reactivated fault. The hydrous phase would essentially decrepitate in the process zone. Note that this possibility would relax the constraint of a preexisting high pore pressure all along the path of propagation.

DENSIFICATION-INDUCED ANTICRACK FAILURE

Discovery of High-Pressure Faulting

During the early 1980s, a controversy developed concerning the mechanism of the olivine-spinel transformation. Experimental evidence was produced favoring both a martensitic (shear) mechanism and a mechanism involving incoherent nucleation and growth of the denser phase. The experiments were conducted in various types of apparatus and on several different chemical systems, all of which exhibit this transformation. At that time it was possible to conduct only a few types of experiments at the extreme pressures under which silicate olivine transforms to β or γ olivine; hence, a variety of analogue materials were used to study the transformation indirectly. Upon review of this literature, Green (1984) proposed that the evidence for both mechanisms was compelling and that the reason for two mechanisms was that those experiments in which a martensitic mechanism was found were conducted under large deviatoric stresses and those in which nucleation and growth occurred were under much smaller stresses. Subsequently, Burnley & Green (1989)

Annu. Rev. Earth Planet. Sci. 1995.23:169-213. Downloaded from www.annualreviews.org
by California Institute of Technology on 06/20/13. For personal use only.

demonstrated the reality of the two mechanisms in Mg_2GeO_4. They conducted constant-strain-rate experiments on an olivine polycrystal in the spinel stability field at pressures of 1–2 GPa. At low temperatures, the specimens were very strong and showed no transformation when viewed in the optical microscope, but transmission electron microscopy demonstrated the existence of thin lamellae of spinel produced by the martensitic mechanism. At high temperatures, the specimens were much weaker because nucleation and growth of the spinel phase occurred easily and quickly on grain boundaries of the olivine.

In the course of those experiments, a faulting instability was discovered in specimens deformed in the narrow temperature window between the regimes in which the two transformation mechanisms operate (Figure 10*a*). Because the specimens deformed at lower temperatures were fully ductile, yet supported stresses much higher than did the faulted specimens (Figure 9*b*), it was clear that the faulting was not due to brittle failure. Hydrostatic experiments under these conditions (1200 K, 1 GPa, < 1 hr) showed no evidence of transformation, but these deformation experiments exhibited spinel in the (often multiple) fault zones and small amounts elsewhere with a distinctive morphology. Scattered throughout the specimens, small crack-shaped lenses of spinel were found extending out from olivine grain boundaries and pyroxene inclusions within the olivine crystals (Figure 10*c,d*). The lenses displayed an extremely strong tendency for their long axes to lie perpendicular to the compression direction (Figure 10*d*; see also Figure 11 of Burnley et al 1991), and the spinel phase within them had a grain size of the order of 10 nm (Figure 10*e*). Specimens taken to the brink of failure but unloaded before faulting could occur displayed the same widely distributed, highly oriented spinel lenses. Within the fault zones themselves the spinel also was extremely fine-grained (Figure 10*f*).

Anticrack Theory of Faulting

Before publication of the definitive work on brittle shear fracture by Lockner et al (1991, 1992), Green & Burnley (Green & Burnley 1989, 1990; Burnley et al 1991) had been struck by the marked similarity between the microstructures of their specimens and those associated with brittle shear fracture. They were particularly impressed that the lenses looked like cracks and that these lenses displayed a very strong preferred orientation in the stress field, opposite to that of tensile cracks. Because the spinel phase is more dense than the olivine phase, the displacements associated with these lenses are the opposite to those involved in opening tensile cracks. As a consequence, it was concluded that these features also are Mode I and must be *anticracks* (Figures 11*a,b*), a concept introduced by Fletcher & Pollard (1981) in an elegant model to explain stylolites (solution seams in sedimentary rocks). These authors showed that all of the equations describing tensile cracks are directly applicable to anticracks, by simply reversing the sign of displacements and stresses. Green & Burnley

Annu. Rev. Earth Planet. Sci. 1995.23:169-213. Downloaded from www.annualreviews.org
by California Institute of Technology on 06/20/13. For personal use only.

(1989, 1990; Burnley et al 1991) surmised that microanticracks must play the same fundamental role in transformation-induced faulting as microcracks do in brittle faulting (Figure 11*c*). Insight into how this might be so was provided by the knowledge that Mg_2GeO_4 spinel with a grain size of a few microns has the property of "superplasticity" under conditions similar to those of Burnley's experiments (Vaughan & Coe 1981). Superplasticity is a weakening property induced by small grain sizes in which a large fraction of the strain is accomplished by grain-boundary sliding, a viscous process. The grain-size-dependence of superplastic materials (Mukherjee et al 1989) suggested that the nanocrystalline spinel in the anticracks should be much weaker than olivine and capable of flowing at very high strain rates. Green and Burnley further postulated that the fine-grained spinel found in the fault zones was fabricated in the anticracks and incorporated into the fault zone during formation and growth of the fault, thereby providing a lubricant for fault movement at high pressure. These characteristics, plus the fact that this instability accompanies a phase transformation known to occur in the mantle under conditions where deep earthquakes occur, led to the anticrack theory of deep-focus earthquakes (Green & Burnley 1989, 1990; Burnley et al 1991).

The theory of faulting as originally put forth by Green & Burnley (1989) postulated the following: (*i*) Under conditions such that the deformation and transformation rates are suitably balanced, rising stress at constant temperature or rising temperature at constant stress induces anticrack growth. (*ii*) At some critical density of anticracks, the material locally loses its ability to support the applied stress because of the assumed very weak contents of the anticracks (due to superplasticity induced by the extremely fine grain size); failure begins by linking up of the anticracks and formation of a protofault. (*iii*) The geometry of the stress concentrations associated with the fault induces enhanced anticrack growth around its margins, thereby continually providing the superplastic lubricant as the fault disk expands. (*iv*) During rapid anticrack growth, sufficient heat is released by the exothermic reaction to raise the local temperature which, in turn, causes the reaction rate to increase, which causes further temperature increase, etc. (*v*) The positive feedback between reaction rate and temperature incites a thermal runaway that causes the fault to grow catastrophically.

Laboratory Tests of the Anticrack Theory

Since formulation of this theory, a series of experimental tests of various aspects of the model have been performed:

1. The experiments in which the mechanism was discovered were conducted on an analogue material, Mg_2GeO_4, not on mantle olivine. Moreover, in the germanate system, olivine transforms directly to the spinel structure (γ olivine), whereas in olivine of mantle composition, there is an intervening

Annu. Rev. Earth Planet. Sci. 1995.23:169-213. Downloaded from www.annualreviews.org
by California Institute of Technology on 06/20/13. For personal use only.

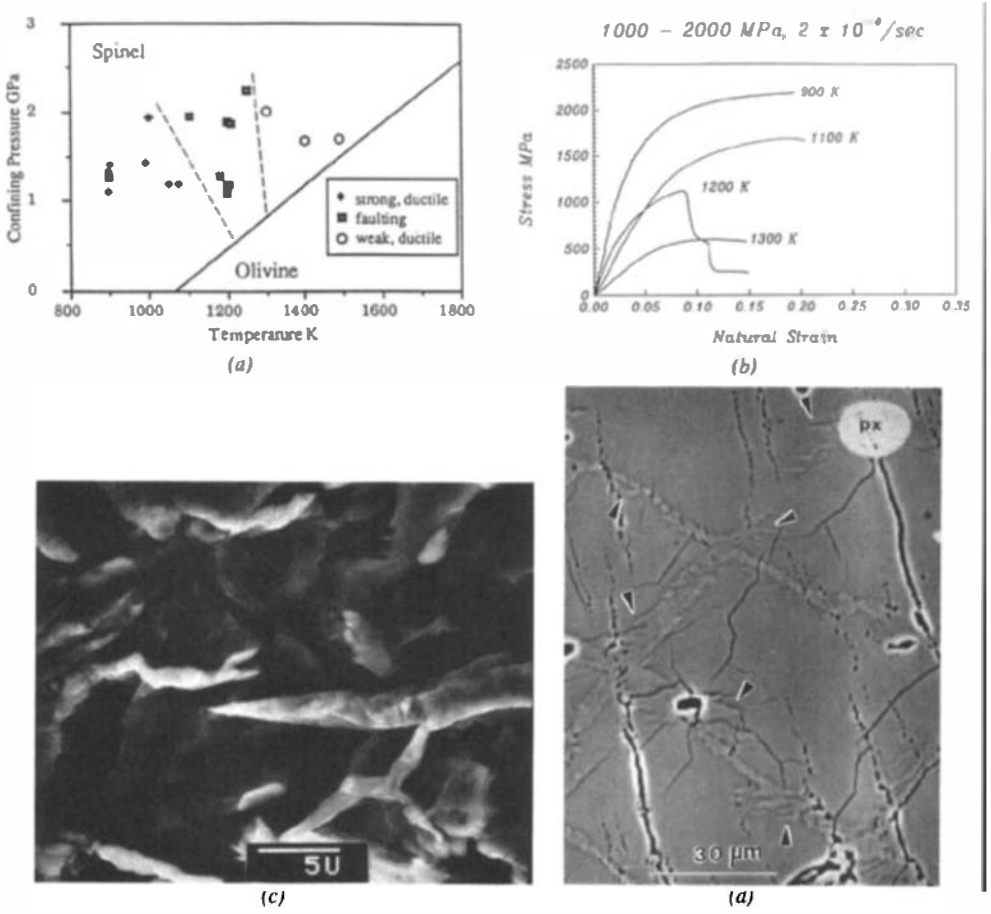

transformation to the spineloid structure (β olivine). In addition, the germanate experiments were conducted at pressures of only 1–2 GPa; however, the silicate transformation occurs in the Earth at 13 GPa (400 km). Although low-pressure experiments on germanates have proven repeatedly to be excellent models for similar processes operating in silicates only at very much higher pressures, previous success involving elastic properties (Liebermann 1975) and static transformation processes (Green et al 1992b) was no guarantee that this complicated process of anticrack growth and faulting was equally well modeled by the germanate system. The initial faulting experiments were conducted on germanate olivine because apparatus did not (and still does not) exist in which one could apply controlled stresses and measure them during deformation at pressures greater than a few GPa. Nevertheless, Green et al (1990) modified D Walker's then-

Annu. Rev. Earth Planet. Sci. 1995.23:169-213. Downloaded from www.annualreviews.org
by California Institute of Technology on 06/20/13. For personal use only.

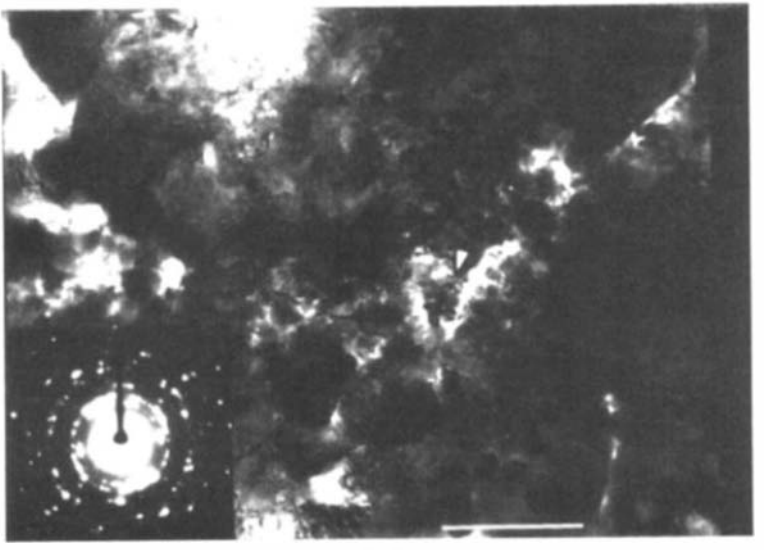

(e)

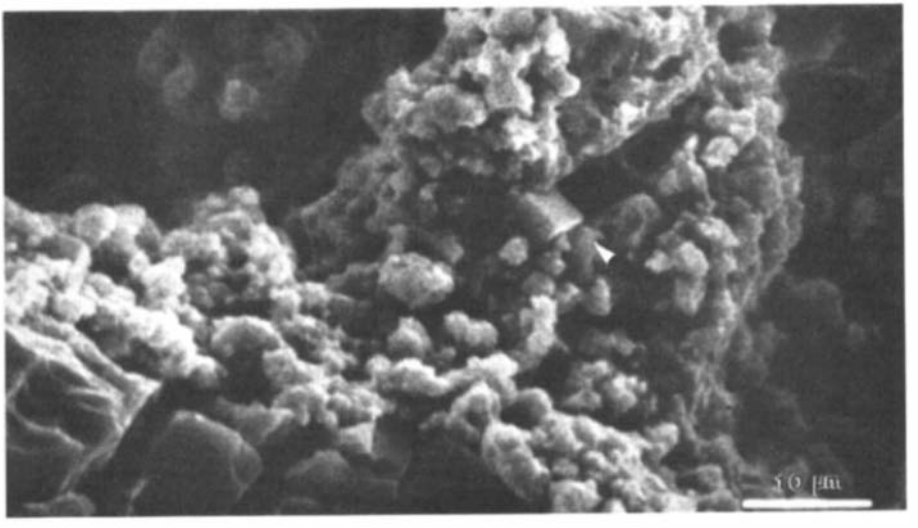

(f)

Figure 10 Characteristics of faulting in Mg_2GeO_4. (*a*) Conditions of faulting (from Burnely et al 1991; phase relations after Ross & Navrotsky 1987). (*b*) Stress-strain curves showing ductile behavior at temperatures above and below the instability (from Green & Burnley 1990). (*c*) SEM of etched specimen showing lens of fine-grained spinel in olivine (modified after Green & Burnley 1989). (*d*) Back-scattered SEM image of lenses (*arrowheads*) growing on olivine subgrain boundaries and a pyroxene inclusion (px). Maximum compressive stress is N-S. (*e*) TEM image and selected-area electron diffraction pattern of extremely fine-grained spinel in lens (modified after Burnley et al 1991); scale bar is 5 μm. (*f*) SEM of etched specimen showing fine-grained spinel and olivine fragment (*arrowhead*) in fault zone (modified after Green & Burnley 1990).

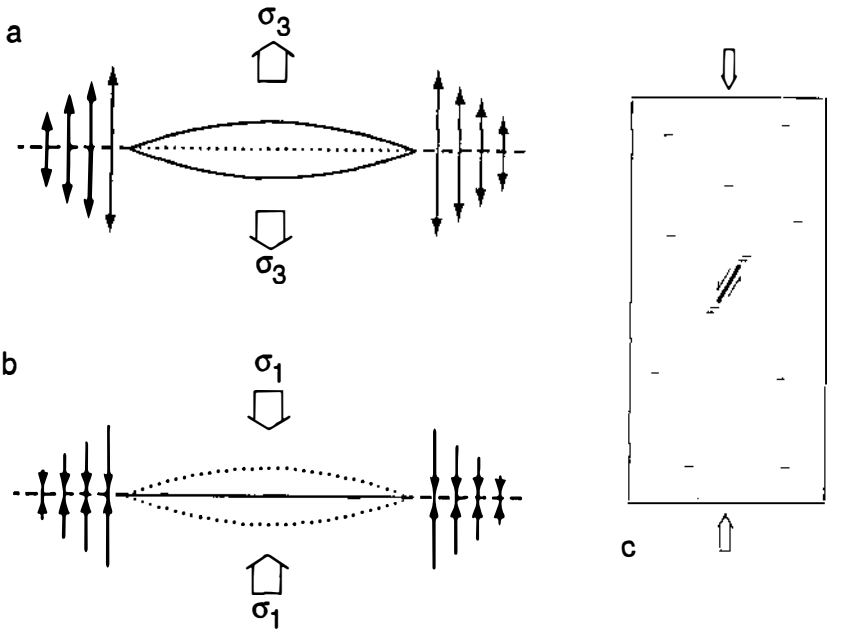

Figure 11 Comparison of Mode I cracks and anticracks. (*a*) A small planar flaw in a solid (*dotted line*) is pulled open by a remote tensile stress, σ_3, yielding a lens-shaped void (crack) with tensile stess concentrations at its tips. (*b*) A small lenticular void (*dotted*) in a solid is pushed closed by a remote compressive stress, σ_1, yielding a compressive stress concentration at its tips. The stress distribution is identical in the two cases except that the algebraic signs have been reversed. This is an empty anticrack. Growth of a denser phase with the geometry shown in (*b*) produces a similar stress pattern (a filled anticrack). (After Green & Burnley 1989.) (*c*) Transformation-triggered faulting with "process zone" of anticracks (compare with Figure 9).

Annu. Rev. Earth Planet. Sci. 1995.23:169-213. Downloaded from www.annualreviews.org
by California Institute of Technology on 06/20/13. For personal use only.

newly-designed multianvil apparatus at the Lamont-Doherty Geological Observatory of Columbia University to apply stresses to olivine of mantle composition while raising the pressure into the β olivine stability field at high temperature. Since they could not measure stresses and could not know in advance the critical conditions under which faulting might occur, they used the characteristic microstructures that develop under stress in germanate experiments (Vaughan et al 1984, Green 1986, Green et al 1992b) as a guide. They were successful and achieved faulting accompanied by anticrack development at 14 GPa (Figure 12). The fault in that experiment propagated through a temperature gradient of perhaps 200 K. This observation shows that the temperature constraints on propagation of a fault initiated by the anticrack mechanism are less stringent than on the nucleation process.

Annu. Rev. Earth Planet. Sci. 1995.23:169-213. Downloaded from www.annualreviews.org
by California Institute of Technology on 06/20/13. For personal use only.

Figure 12 Photomicrograph taken between crossed polarizers of silicate specimen faulted at 14 GPa during the $\alpha \rightarrow \beta$ olivine phase transformation. Asterisks mark a crystal severed by the fault; the high-density phase filling the fault zone and growing on grain boundaries is labeled β; arrows point to anticracks filled with the β phase. (Modified after Green et al 1990.)

2. The small size of the specimens involved in the faulting experiments and their position deep within the high-pressure apparatus precluded hearing an audible signal during faulting. Obviously, any mechanism proposed to explain earthquakes must radiate sonic energy. To test this aspect of the process and to further investigate the self-organizing properties of anticrack faulting, Green collaborated with C Scholz to modify the high-pressure deformation apparatus to make it more quiet and to facilitate detection of acoustic emissions (Scholz 1990). Their results (Green et al 1992a, Tingle et al 1993) showed that seismic energy is generated during faulting but not during anticrack growth (Figure 13*a,b*).

3. These same workers measured the pressure-dependence of the stress at which the specimens failed and of the resistance to sliding on the faults

Annu. Rev. Earth Planet. Sci. 1995.23:169-213. Downloaded from www.annualreviews.org by California Institute of Technology on 06/20/13. For personal use only.

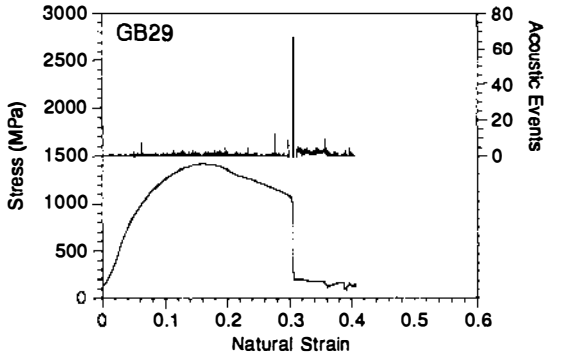

(a)

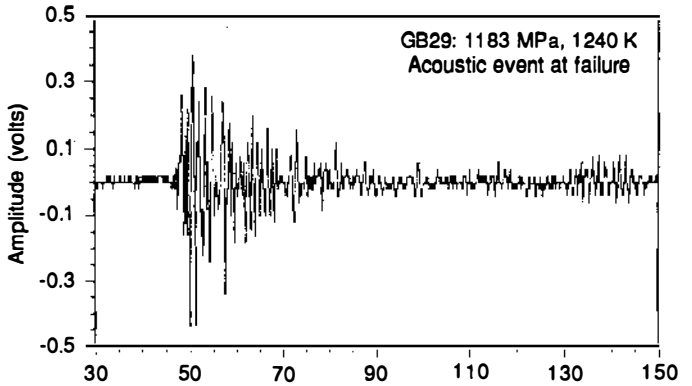

(b)

Figure 13 (a) Stress-strain curve showing faulting and acoustic emissions in Mg_2GeO_4. (*b*) Wave form from two acoustic events during failure. (From Tingle et al 1993.)

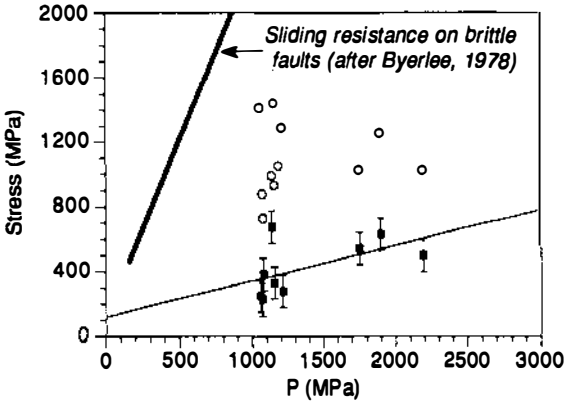

Figure 14 Pressure-dependence of faulting (*open symbols*) and sliding resistance on faults (*closed symbols*). Heavy line shows pressure-dependence exhibited by frictional faults. (From Tingle et al 1993.)

after their creation (Tingle et al 1993; Figure 14). No pressure-dependence of failure strength was found. Because this instability is critically dependent on achieving a balance between the rate at which deformation is imposed and the rate at which the transformation is initiated (Burnley et al 1991), small differences from specimen to specimen induced considerable scatter in the failure stress. Nevertheless, the results were clearly incompatible with the pressure-dependence expected for brittle failure (Scholz 1990). The pressure-dependence of the sliding resistance was much more tightly constrained and was considerably less than that of frictional processes. The small pressure-dependence was consistent with that expected for a viscous process. Once a fault had been created, the stress on the specimen required to move it was about 1/3–1/4 of the maximum stress supported by the specimen in the early part of the experiment. That maximum strength provides a good measure of the crystal-plastic flow stress of the olivine phase under the conditions of faulting: Thus, the fine-grained spinel of the fault zones is much weaker than the olivine. This observation was in stark contrast to the rheology of coarser-grained aggregates of the spinel phase synthesized from the same material, in which the spinel phase was found to be twice as strong as the olivine phase under the same conditions (Tingle et al 1991). These results require that the weakness of the spinel in the fault zones was produced by its very fine grain size, which confirms the superplastic behavior of spinel hypothesized in the anticrack theory.

Transmission electron microscopy of the silicate specimen in which faulting was produced strongly suggested that β olivine is also stronger than olivine under the conditions of that experiment (Dupas et al 1994). Bussod et al (1994) have also produced evidence for this under similar conditions. These

Annu. Rev. Earth Planet. Sci. 1995.23:169-213. Downloaded from www.annualreviews.org by California Institute of Technology on 06/20/13. For personal use only.

results confirm superplastic behavior of the anticrack and fault-filling material in the silicate system under conditions of the mantle transition zone.

4. To test the hypothesis that a thermal runaway is required for anticrack growth to be sufficiently rapid for catastrophic fault propagation, Green & Zhou (1994) deformed a $CdTiO_3$ ilmenite polycrystal in the perovskite stability field. The volume and entropy changes, ΔV and ΔS, during this densification reaction are almost identical to those for the olivine-spinel reaction in Mg_2GeO_4, except for the important difference that the sign of ΔS is reversed, i.e. the reaction is endothermic rather than exothermic. Thus, the prediction was that ilmenite would transform to perovskite without producing faulting. Green & Zhou performed a series of experiments ranging from conditions where the temperature was too cold for the reaction to run, to conditions where nucleation and growth occurred readily (Figure 15*a*). Transformation proceeded uneventfully; neither anticracks nor faulting were observed. These experiments were consistent with the anticrack faulting theory in that they demonstrated that this endothermic reaction is incapable of generating an instability, but they could not be considered definitive because they provide no proof of the generality of this observation. However, these authors then reasoned that, although the theory requires that the sign of ΔS be positive (Figure 15*b*), there is nothing that should require that the sign of ΔV be negative to allow failure. Therefore, they reversed the procedure and deformed perovskite polycrystals in the ilmenite stability field, again under conditions from below the onset of transformation to the point of extensive transformation. In this case, deformation during rapid transformation yielded ductile flow at a stress much below that of the strength of either phase, and deformation on the threshold of transformation produced multiple faults, all with ilmenite in the fault zone (Figure 15*c*). In the faulted specimen, lenses of ilmenite parallel to the compression direction were found distributed throughout the specimen (Figure 15*d*). Thus, transformation-triggered faulting was produced during this exothermic reaction, but this time, because ΔV was positive, the lenses were "cracks" parallel to the compression direction instead of anticracks perpendicular to it. Importantly, as had been found previously in the $\alpha \rightarrow \beta$ and $\alpha \rightarrow \gamma$ olivine faulting, lenses and transformation went hand in hand; when lenses did not develop, neither did faults lined with the new phase.

5. Potentially the same mechanism operates in the ice Ih $\rightarrow$ II transformation (Kirby et al 1991). Only indirect evidence for the high-pressure phase has been documented in this system, and the inferred anticracks are 1–2 orders of magnitude larger than in the germanate, silicate, and titanate systems, but the correlation of these microstructures with faulting of metastable ice Ih in the ice II stability field suggests that the same process operates.

Annu. Rev. Earth Planet. Sci. 1995.23:169-213. Downloaded from www.annualreviews.org
by California Institute of Technology on 06/20/13. For personal use only.

Annu. Rev. Earth Planet. Sci. 1995.23:169-213. Downloaded from www.annualreviews.org
by California Institute of Technology on 06/20/13. For personal use only.

These experimental tests of the anticrack faulting theory greatly expand knowledge of the processes involved and provide strong support for the original concept. The process operates in mantle olivine under mantle conditions and generates seismic waves during faulting, the fine-grained denser phase is superplastic, and an endothermic reaction is incapable of triggering faulting. There are now two systems in which this latter point has been shown—$CdTiO_3$ perovskite-ilmenite, and Mg_2GeO_4 olivine-spinel. [Burnley's original germanate experiments also included some experiments on the spinel → olivine reaction that developed neither lenses nor faulting, but no significance was attached to that observation at the time (Burnley 1990).] Of particular importance in these more recent experiments is the one-to-one correspondence demonstrated between development of lenses of the new phase and transformation faults. This correspondence strongly suggests that the fundamental instability is inherent in lens growth rather than fault growth. This latter point is the first significant modification that has had to be made in the anticrack theory of faulting since its original formulation. The original concept had been that runaway lens growth occurred only during the organization and propagation of the fault; prefaulting anticracking was viewed as stable. Lack of acoustic emissions preceding failure seemed to be consistent with that view. However, the development of lenses only in the exothermic direction in both systems thus far investigated requires that concept to be revisited. For example, the data clearly show that both faulting and the development of lenses are insensitive to the sign of ΔV of the transformation, and they both require that ΔS be negative. Lastly, the $CdTiO_3$ experiments establish firmly that the transformation faulting mechanism is fully analogous to brittle faulting. Both are self-organizing, both exhibit fundamental instability in the Mode I features (i.e. displacements are perpendicular to the plane of the feature), and both require a working "fluid" to operate at high pressure.

Geophysical Implications

The remarkable macroscopic similarity between these two microscopically very different failure mechanisms helps explain the great similarity between deep and intermediate (and shallow!) earthquakes. Until recently, this similarity has been thought to be evidence against the existence of two mechanisms. That argument is no longer viable because to a first order, one should expect the same signal from both of these now well-documented faulting mechanisms. The earthquake signal is dominated by the sudden shearing displacement across the fault, whether it be during fault creation or reactivation. Therefore, everything related to the geometrical aspects of this part of the signal should be similar for both mechanisms. On the other hand, no explanation is yet in hand as to why the range of stress drops should be the same for both mechanisms. Also, one might expect the earliest and latest parts of the seismic signal to

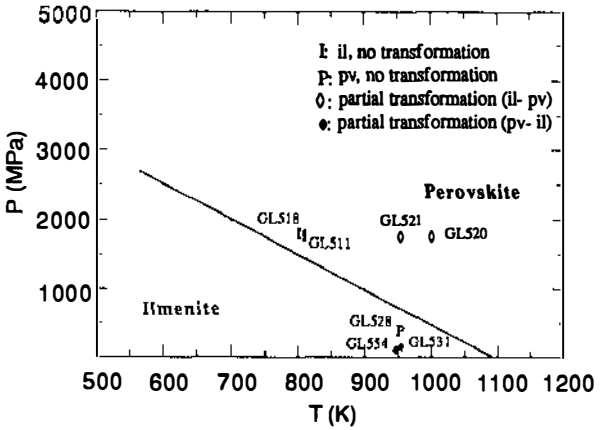

(a)

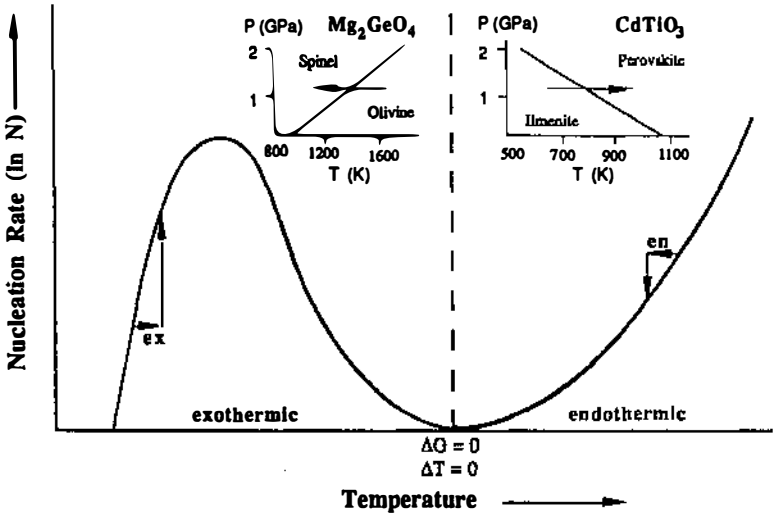

(b)

carry some information about the microphysics. For example, the initiation of faulting could occur at different rates for the two mechanisms due to differences in viscosity between pore fluid and superplastic solid. Similarly, the waning stages of the earthquake could reflect the rheology of the fault zone, which is different in the two mechanisms. As we summarized above, recent results in analysis of the seismic signal from deep and intermediate earthquakes suggest that such diagnostic information may be contained in the early and late portions of the signal, but interpretation of those data in terms of mechanism is not straightforward.

Annu. Rev. Earth Planet. Sci. 1995.23:169-213. Downloaded from www.annualreviews.org
by California Institute of Technology on 06/20/13. For personal use only.

Annu. Rev. Earth Planet. Sci. 1995.23:169-213. Downloaded from www.annualreviews.org
by California Institute of Technology on 06/20/13. For personal use only.

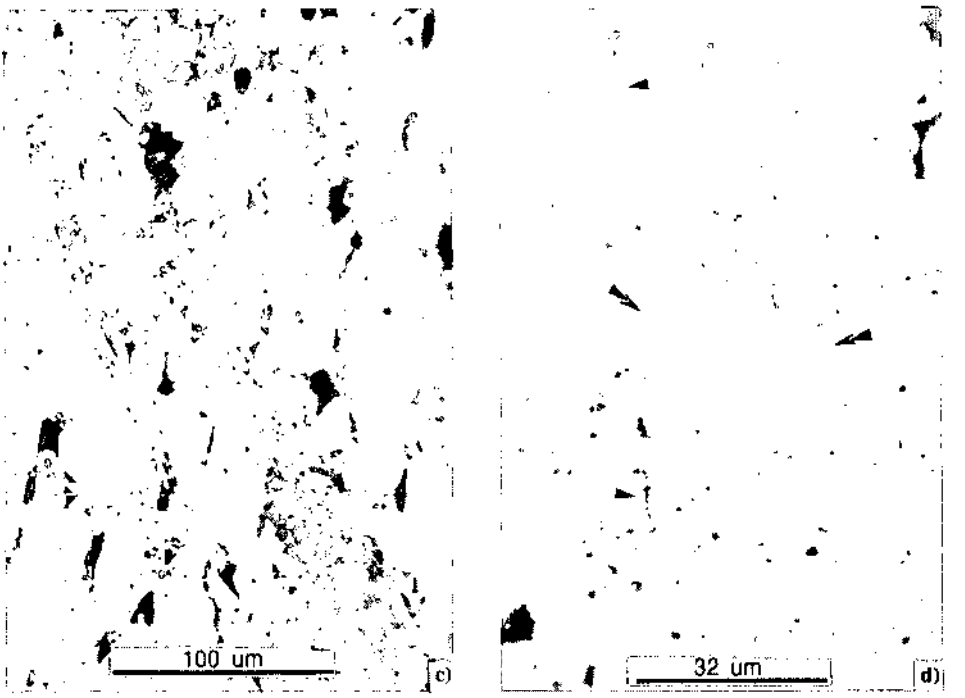

Figure 15 Transformation-induced faulting in $CdTiO_3$. (*a*) Phase diagram showing experimental conditions (phase relations from Liebertz & Rooymans 1965). (*b*) Thermodynamics of nucleation rate showing the fundamental difference between an exothermic reaction (down-temperature) with two limbs to the curve and an endothermic reaction (up-temperature) with only one limb to the curve. See text for discussion. (*c*) Reflection optical micrograph showing ilmenite (*dark gray*) lining a fault zone in perovskite. Black areas are surface imperfections. (*d*) Mode I ilmenite-filled lenses (*double arrowheads*) in perovskite. Note also the presence of open Mode I cracks (*arrowheads*) parallel to ilmenite "cracks." (All panels from Green & Zhou 1994.)

MODEL OF INTERMEDIATE-FOCUS EARTHQUAKES

As discussed above, the vast majority of earthquakes deeper than 30 km occur in subduction zones. Furthermore, either a fluid is required to enable brittle failure or frictional sliding, or some other mechanism is required, such as transformation-induced faulting. The latter mechanism is not restricted to olivine and its polymorphs, as evidenced by its occurrence in $CdTiO_3$ and its probable operation in H_2O ice. However, the only polymorphic transformation known to occur in any of the major minerals of the oceanic crust and mantle under conditions present in the upper mantle above 400 km is the ortho-clino inversion in enstatite. This transformation occurs by a martensitic mechanism (Coe & Kirby 1975) that could, in principle, emit a seismic signal (Meade &

Annu. Rev. Earth Planet. Sci. 1995.23:169-213. Downloaded from www.annualreviews.org
by California Institute of Technology on 06/20/13. For personal use only.

Jeanloz 1989), but since enstatite never constitutes more than about 30% of the oceanic lithosphere, it could not give rise to significant earthquakes. Moreover, that transformation occurs stably at about 250 km (Pacalo & Gasparik 1990), in the middle of the smooth exponential decrease in the frequency vs depth relation (Figure 2). Facies changes such as spinel to garnet peridotite or basalt to eclogite represent pressure-driven metamorphic reactions, not transformations, and are incapable of generating faulting instabilities. In both cases, these facies changes involve reconstructive reactions between multiple parent and daughter minerals. Such reactions require diffusion to take place on the scale of millimeters—a process too slow to allow faulting on a time scale appropriate for an earthquake. Therefore, at this time it is difficult to envision any mechanism for intermediate-focus earthquakes other than pore-pressure-enabled reactivation of old faults created near the surface, or generation of new faults by the same process.

In addition to these arguments that appear to rule out other mechanisms, there are many positive reasons to conclude that fluid-induced fault movement is responsible for earthquakes at intermediate depths: 1. It is known from many lines of evidence that H_2O is carried down as connate water in sediments on the top of subducting slabs (e.g. B and ^{10}Be contents of arc magmas, composition of arc magmas, H_2O in fluid inclusions in arc and back-arc magmas, and generation of the arc magmas themselves in the mantle wedge above the slab—Sakuyama 1983, Tatsumi et al 1986, Morris & Tera 1989, Ryan & Langmuir 1993, Stolper & Newman 1994). 2. Studies of ocean dredge samples and ophiolites show that widespread hydrothermal alteration of the oceanic crust takes place, with lesser alteration of the mantle immediately underlying it (Alexander et al 1993, Gillis et al 1993, Nehlig et al 1994, Bettison-Varga et al 1994). Such alteration falls off rapidly with depth; xenoliths from the suboceanic mantle show very little evidence of hydration. A minority of these xenoliths show veins or scattered crystals of amphibole or phlogopite, but the vast majority consist of coarse-grained peridotites with clean grain boundaries; they show no evidence of having contained a hydrous phase that might have decomposed during the residence time of the xenolith in the magma. 3. Normal faulting occurs in the shallow lithosphere where it bends and turns downward into the subduction zone. Any of those faults that cut the surface could provide access for water to produce hydrous alteration along them. 4. The smooth trend of the earthquake frequency curve down to 300 km suggests that the faulting mechanism remains the same all the way to that depth. These observations plus the compelling laboratory evidence for dehydration embrittlement (Raleigh & Paterson 1965, Meade & Jeanloz 1991) make this mechanism very favorable for intermediate-depth earthquakes.

The exponential decline in earthquake frequency of more than two orders of magnitude suggests that the underlying cause of the instability is becoming

exhausted. The latter inference is consistent with the observed migration of earthquakes into the slab with increasing depth (Hasegawa et al 1978, Matsuzawa et al 1990), coupled with the concentration of hydration near the top of the lithosphere and the progressive inward migration of isotherms as the slab heats slowly with depth. The observation of double seismic zones with spacings up to 40 km at intermediate depths (Hasegawa et al 1978, Matsuzawa et al 1990) is not immediately explained by this scenario (e.g. Glennon & Chen 1994), but may be related to reactivation of deep faults that were hydrated at shallow depths.

We conclude that dehydration embrittlement is the cause of intermediate-focus earthquakes. The majority of water that goes down with the slab is in the crust and sediments and is lost to the mantle wedge above the slab where it induces arc and back-arc melting. Most of the remainder is along faults and is slowly cooked out as the slab warms and induces a decreasing population of earthquakes that continues to about 300 km. Any H_2O remaining in the slab at this depth probably is dissolved in the pyroxenes and olivine (Thompson 1992, Bell & Rossman 1992), and becomes unavailable for faulting.

MODEL OF DEEP-FOCUS EARTHQUAKES

Meade & Jeanloz (1991) proposed that hydrous phases are present to depths of about 12 km and could remain present metastably in the cold interior of slabs, enabling earthquakes at all depths. They based their arguments on their observation of acoustic emissions in compressed serpentinite to pressures of 25 GPa (equivalent to 700 km depth). They correlated the acoustic emissions with dehydration to 9 GPa and with amorphization at higher pressures. The recent demonstration that intermediate and deep earthquakes occur much deeper into the slab than 12 km invalidates the specific model of Meade & Jeanloz, but the possibility of hydration along faults to greater depths in the slab leaves the possibility open that dehdyration embrittlement could be responsible for these earthquakes. However, experimental studies of dehydration reactions suggest that it is unlikely that these reactions could be inhibited above about 700 K (Navrotsky & Bose 1994), restricting to intermediate depths earthquakes triggered by this mechanism. Stable preservation of hydrous phases along a slab geotherm to depths at which some of the recently discovered very high pressure hydrous phases could be stable is not ruled out by experimental data (Navrotsky & Bose 1994), but requires extended optimistic extrapolation of known relations. We therefore conclude that although there is a high probability that intermediate-focus earthquakes are induced by dehydration of hydrous phases, it is unlikely that dehydration contributes significantly to deep earthquakes.

Only two criteria must be fulfilled for production of the secondary, deeper, population of earthquakes (300–680 km; Figure 2) by the anticrack mechanism:

Annu. Rev. Earth Planet. Sci. 1995.23:169-213. Downloaded from www.annualreviews.org by California Institute of Technology on 06/20/13. For personal use only.

Annu. Rev. Earth Planet. Sci. 1995.23:169-213. Downloaded from www.annualreviews.org
by California Institute of Technology on 06/20/13. For personal use only.

the presence of shear stress (evidenced by the existence of double-couple earthquakes) and the presence of metastable olivine. In experiments in the diamond-anvil cell, Sung & Burns (1976) and Sung (1979) examined the kinetics of transformation of olivine to spinel by the nucleation and growth mechanism. They concluded that the temperature in the interior of rapidly subducting slabs probably would be too cold for olivine to transform to its denser polymorphs when it was carried out of its stability field. The kinetics of the olivine-spinel transformation have been further investigated extensively by D Rubie and coworkers (Rubie et al 1990, Rubie 1993, Rubie & Ross 1994) in a multianvil apparatus that allows recovery and study of much larger specimens than does the diamond-anvil cell. These studies support the earlier conclusions of Sung & Burns that metastable transport of olivine out of its stability field is to be expected in cold slabs. Moreover, Rubie & Ross (1994) emphasized that progression of bulk transformation will be controlled by growth rates rather than nucleation rates. The experiments on Mg_2GeO_4 (Burnley et al 1991) showed that both nucleation and growth rates are extremely slow under hydrostatic conditions at the temperature of the faulting instability. The action of stress was to produce greatly enhanced nucleation rates locally in the form of anticracks. Combining these two sets of data suggests that the faulting instability in the mantle should begin at a temperature just slightly below that for the onset of transformation under hydrostatic stress and should continue in a narrow temperature range in which bulk transformation of up to perhaps 30% occurs (the maximum degree of transformation that could occur and still allow the faulting instability is not yet well constrained experimentally). Rubie & Ross (1994) suggest onset of the transformation under natural conditions to be at a temperature of 850 ± 50 K. Recent results by PC Burnley (personal communication, 1993) suggest that the temperature at which transformation begins in Mg_2GeO_4 is insensitive to pressure even with very large overstepping of the phase boundary. We therefore conclude that the best guess currently available for the critical temperature range for anticrack faulting in the Earth is between 850 and 1000 K. These temperatures are significantly lower than the maximum suggested by Sung (1979), but still consistent with modern thermal models of subduction zones (e.g. Helffrich et al 1989, Iidaka & Furukawa 1994). If the kinetics of onset of the transformation are controlled by the homologous temperature rather than the absolute temperature, the critical conditions for faulting could be at somewhat higher temperature at greater pressures. This is an important matter for future research.

Sung & Burns (1976) correctly concluded (as had others before them, e.g. Bridgman 1945) that the presence of a wedge of cold lithosphere containing metastable olivine provides the opportunity for earthquake generation. However, like their predecessors, their vision was that nucleation of the stable phase deep within its stability field would lead to runaway transformation,

Annu. Rev. Earth Planet. Sci. 1995.23:169-213. Downloaded from www.annualreviews.org by California Institute of Technology on 06/20/13. For personal use only.

and they concluded that deep earthquakes would be implosions—a prediction not compatible with seismic evidence. Vaisnys & Pilbeam (1976), in a theoretical study, suggested that as well as runaway implosion, transformation of metastable olivine might trigger a shear instability in the presence of a shear stress if the transformation could be organized appropriately. Kirby (1987) made a similar suggestion based in part on his early experiments on ice. Yet, several pieces of the puzzle were still missing: demonstration of the high-pressure phase in association with the instability, determination that it operates only under a specific set of conditions, and discovery of the self-organization process. The early germanate faulting experiments provided those crucial ingredients and made it possible to construct a predictive model that could be tested. The early model of Green & Burnley (1989) has now been subjected to a variety of experimental and seismological tests, leading to the model presented below.

In lithosphere undergoing rapid subduction, olivine is carried out of its stability field at temperatures too cold for the reaction to run. However, as the slab heats up, the particle path of the metastable olivine must eventually intersect the conditions under which the transformation begins (here assumed to be 850 K and independent of pressure; Figure 1). Anticrack faulting can begin at this temperature if the slab is under sufficient stress. The details of exactly when (or if) the instability will be triggered depend on a subtle interplay between the imposed deformation rate (produced by the local stress) and the rate of temperature increase experienced along the particle path. (If the material gets transported up the temperature gradient too quickly, normal nucleation and growth can be sufficiently rapid to accelerate the rates of bulk transformation and stress relief, thereby enabling the material to avoid the instability altogether.) It follows that the model predicts seismic zones along both margins of the metastable wedge if the stress fields are appropriate and if the temperature gradients at both the upper and lower surfaces are appropriate to lead to the critical conditions. At the time of formulation of the anticrack theory of deep earthquakes (Green & Burnley 1989), deep, double seismic zones were unknown, but two recent studies have detected such zones in deep environments (Wiens et al 1993, Iidaka & Furukawa 1994). The latter study is in the same portion of the Izu-Bonin subduction zone where Iidaka & Suetsugu (1992) previously proposed the presence of a metastable olivine wedge based on comparison of seismic velocity models with observed travel times of waves traveling up the slab. The observation of a double seismic zone bounding a metastable olivine slab confirms a specific prediction of the anticrack theory and thus provides strong support for the theory.

When the material reaches the critical conditions, fault nucleation occurs and propagation begins. Fault growth will continue until the fault reaches a region of insufficient stress to maintain the instability, a region where the

transformation to β or γ olivine has already occurred, or a region where the temperature is too cold to allow continuation of the process. The results from the silicate experiment of Green et al (1990) suggest that the temperature range could be as much as 200 K. In a recent study, Glennon & Chen (1994) made detailed analyses of eight deep earthquakes in the Kurile and Izu-Bonin arcs, and found that the four that exhibit directivity originated deep within the slab and propagated toward its top surface. In particular, they modeled the September 28, 1988 earthquake (480 km depth) in the Izu-Bonin slab as traveling 31 ± 8 km westward in a subhorizontal plane, with the component perpendicular to the Wadati-Benioff zone being 28 ± 7 km. This latter dimension is indistinguishable from the 20–25 km spacing of the two seismic zones at depths of 300–400 km in this slab (Iidaka & Furukawa 1994). Glennon & Chen inferred from the orientation and length of this fault that it originated on the lower boundary of the metastable olivine wedge (Iidaka & Suetsugu 1992), propagated completely across it, and stopped where the transformation is complete on the other side.

Above we discussed the systematics of stress distributions as a function of depth in subducting slabs, and drew attention to the difficulty in explaining them with the thermo-mechanical model popular in the 1970s and 1980s. In contrast to that model, the transformation-triggered faulting mechanism carries implicit in it the generation of stresses due to the presence of the metastable olivine wedge. In a warm slab, there is no metastable wedge because transformation occurs uneventfully at the equilibrium phase boundary. Shallowing of the transformation in the slab provides a significant additional negative buoyancy at 300–400 km, whereas the metastable wedge in cold slabs contributes positive buoyancy in the transition zone. The additional slab pull in "equilibrium" slabs may be responsible for the down-dip tensional focal mechanisms in slabs lacking deep seismicity. Transformation-triggered faulting may also be consistent with the stresses observed in the South America subduction zone despite the down-dip tension at intermediate depths. Engebretson & Kirby (1992) proposed that the subducting Nazca plate contains lithosphere of two ages, due to reorganization of seafloor spreading, with old, cold lithosphere at depths greater than about 500 km. Such a configuration could explain the down-dip tensional stresses of the intermediate events as caused by slab pull associated with an elevated equilibrium transition, followed by a marked seismicity gap, and finally the deep seismicity by anticrack faulting in an isolated region of cold metastable olivine.

The presence of the metastable wedge also offers an alternative possibility for slab-parallel compressional focal mechanisms for deep earthquakes. An idealized subducting slab with a metastable olivine wedge such as shown in Figure 1 will be subjected to regionally coherent stresses simply as a result of that geometry (Goto et al 1987, Kirby et al 1991). Transformation leads to a reduction in volume; hence, the transformed carapace around the metastable

Annu. Rev. Earth Planet. Sci. 1995.23:169-213. Downloaded from www.annualreviews.org by California Institute of Technology on 06/20/13. For personal use only.

Annu. Rev. Earth Planet. Sci. 1995.23:169-213. Downloaded from www.annualreviews.org
by California Institute of Technology on 06/20/13. For personal use only.

wedge will have shrunk relative to the wedge within it, leading to down-dip compression within the wedge (and down-dip extension in the carapace). Transformation-induced superplasticity and normal dislocation creep will lead to significant relaxation of the stresses that can be calculated from the volume change [hence the magnitude of the stresses calculated by Goto et al (1987) are much too large]. However, the vast majority of the denser material in the carapace will be sufficiently coarse-grained to place it in the dislocation creep regime; consequently, it will be inherently stronger than olivine, and the stresses on the metastable wedge will relax slowly. On the other hand, the carapace will be warmer than the metastable wedge, which compensates at least in part for the greater inherent strength of the denser phases. Quantitative modeling of these competing effects must await better rheological data, but it is clear that the metastable wedge must experience slab-parallel self-stresses, consistent with the focal mechanisms generally observed in deep subduction zones. These stresses provide a natural explanation (Kirby et al 1991) for earthquakes that occur in horizontal and/or detached slabs for which there is no obvious source for tectonic stresses [e.g. deep seismicity in Izu-Bonin (van der Hilst et al 1991) and deep seismicity beneath the Fiji Basin (Okal & Kirby 1993)]. Slab-parallel compression for whatever reason indicates that the rocks will be flowing continually and the slab will thicken. Indeed, seismic studies of deep slabs indicate that the cold velocity anomaly thickens at depth (e.g. Grand 1994). Thickening of the metastable wedge by this process will at least in part compensate for thermal narrowing and thereby contribute to preservation of the wedge to great depth (Figure 1*b*).

The temperature distribution in subducting slabs depends on the age of material being subducted and the rate of subduction. Implicit in the anticrack theory is a series of predictions about the variation of deep seismicity with these temperature differences. Obviously, if the slab is sufficiently warm that olivine transforms directly to β olivine at the phase boundary, then earthquakes by this mechanism are precluded; any deep earthquakes occurring in such a slab must be caused by dehydration embrittlement or some other, unknown, mechanism. In a moderately warm slab, metastable persistence of olivine may extend for a distance into the transition zone, but earthquakes should cease at the depth where the central core warms to the critical conditions. The oldest, fastest, slabs should be expected to display earthquakes to the greatest depths. Kirby et al (1991) have shown that the deepest earthquakes in individual subduction zones correlate well with inferred temperature of the slab in just the way predicted.

Cold slabs are sufficiently strong to support the stresses required for earthquakes to depths exceeding the observed seismicity cutoff at 680 km (e.g. Brodholdt & Stein 1988), and at least some slabs are known to penetrate into the lower mantle; therefore, factor other than temperature appears responsible for earthquake termination at the base of the transition zone. The anticrack

Annu. Rev. Earth Planet. Sci. 1995.23:169-213. Downloaded from www.annualreviews.org
by California Institute of Technology on 06/20/13. For personal use only.

theory predicts, and the titanate experiments confirm, that anticrack faulting is impossible during an endothermic transformation; hence, the endothermic decomposition of γ olivine to perovskite + magnesiowüstite is incapable of generating earthquakes. Although the direct decomposition of olivine to the lower-mantle assemblage is exothermic (A Navrotsky 1994, personal communication), it is still unlikely to produce an instability because separation of the olivine molecule into the stable phases requires diffusion on the scale of the grain size of the new phase; the kinetics of diffusion preclude the process from running fast enough to propagate a fault.

The tendency of the largest deep earthquakes to occur in isolation from or near the perimeter of other seismicity can be understood in the context of the anticrack faulting model. In this model the perimeter of the earthquake zone is interpreted to be the boundary of the metastable olivine wedge—hence these regions should have larger volumes of material at or near the critical conditions for faulting than elsewhere. Thus, at any given time, more material is ripe for faulting, and a fault, once initiated, might be expected to run further. In this connection, Houston (1993) pointed out that the geometry of permissible fault planes may be more restricted in such regions and a problem arises concerning sufficient source region to generate large earthquakes. She suggested that these restrictions might lead to simultaneous faulting on multiple faults (oriented such that the associated focal mechanisms have similar compressive axes) and thereby provide a reason why the CLVD component of large deep earthquakes tends to be larger than for other earthquakes. Anticrack faulting in the laboratory frequently produces such multiple faults (Burnley et al 1991).

Another potential connection between the laboratory and the seismic signature of deep earthquakes is the difference in the shape of the envelope (Figure 5) and, hence, the style of rupture for deep and intermediate earthquakes found by Houston & Vidale (1994). The anticrack theory for deep earthquake generation predicts that anticrack faulting should occur only on new faults in untransformed regions, because after faulting stops, the spinel will coarsen to a grain size that is no longer superplastic and the fault is, therefore, unable to slip again. New faults would likely be more homogeneous structures than the reactivated faults, which may be associated with fluid-assisted failure at intermediate depths, and such homogeneous structures would lead to more symmetric earthquake envelopes (e.g. Figure 6).

SUMMARY

For seventy years, the conundrum of how earthquakes can occur at depths of more than a few tens of kilometers has been a major question in geophysics. Modern techniques in seismology and high-pressure mineral and rock physics have now provided a framework in which more detailed answers can be sought. The bimodal distribution of earthquakes with depth implies either two different

failure mechanisms for earthquake generation or a minimum in the driving force for earthquakes (the stress). Although earlier analysis of this problem suggested that the latter might be a reasonable explanation, the much more extensive information now available no longer allows such a simple interpretation. By contrast, our interpretation of the bimodality of the depth distribution as due to two mechanisms is now supported by large amounts of both experimental and seismic data. The restriction of widespread hydration of the oceanic lithosphere to shallow depths, and the kinetics of dehydration reactions observed in the laboratory, strongly suggest that the exponential decrease of earthquakes from the surface to 300 km is due to the progressive decrease in activity of the dehydration embrittlement mechanism as the lithosphere slowly warms by conduction. The anticrack mechanism and its metastable olivine wedge provide a natural explanation for the pattern of stresses observed at intermediate depths, for the rise and fall of the deeper population of earthquakes at exactly the depths at which it appears and disappears, for why deep seismicity is restricted to colder slabs, and for generation of earthquakes in detached or recumbent slabs where there is no evidence of tectonic stresses. Detection of the metastable wedge beneath Japan and double seismic zones there and in Tonga provide the first direct evidence of the operation of this mechanism. Future work coupling laboratory experiments and seismic observations promises to provide a resolution to the remaining issues surrounding this long-standing question.

Any *Annual Review* chapter, as well as any article cited in an *Annual Review* chapter, may be purchased from the Annual Reviews Preprints and Reprints service.
1-800-347-8007; 415-259-5017; email: arpr@class.org

Annu. Rev. Earth Planet. Sci. 1995.23:169-213. Downloaded from www.annualreviews.org by California Institute of Technology on 06/20/13. For personal use only.

Literature Cited

Abe K. 1982. Magnitude, seismic moment and apparent stress for major deep earthquakes. *J. Phys. Earth* 30:321–30

Abers GA. 1992. Relationship between shallow- and intermediate-depth seismicity in the eastern Aleutian subduction zone. *Geophys. Res. Lett.* 19:2019–22

Akaogi M, Ito E, Navrotsky A. 1989. Olivine-modified spinel-spinel transitions in the system Mg_2SiO_4-Fe_2SiO_4: calorimetric measurements, thermochemical calculations, and geophysical applications. *J. Geophys. Res.* 94(15):671–868

Alexander RJ, Harper GD, Bowman JR. 1993. Oceanic and fault-controlled subseafloor hydrothermal alteration in the sheeted dike complex of the Josephine ophiolite. *J. Geophys. Res.* 98:9731–59

Apperson KD, Frohlich C. 1987. The relationship between Wadati-Benioff zone geometry and P, T and B axes of intermediate and deep focus earthquakes. *J. Geophys. Res.* 92:13,821–31

Bell DR, Rossman GR. 1992. Water in Earth's mantle: the role of nominally anhydrous minerals. *Science* 255:1391–97

Benioff H. 1963. Source wave forms of three earthquakes. *Bull. Seismol. Soc. Am.* 53(5):893–903

Bettison-Varga L, Schiffman P, Janecky D. 1994. Fluid-rock interaction in the hydrothermal upflow zone of the Solea Graben, Troodos ophiolite, Cyprus. In *Low Grade Metamorphism of Mafic Rocks*, ed. P Schiffman, HW Day. Geol. Soc. Am. Pap. 296. In press

Bridgman PW. 1936. Shearing phenomena at high pressure of possible importance for geology. *J. Geol.* 44:653–69

Bridgman PW. 1945. Polymorphic transitions and geological phenomena. *Am. J. Sci.* 243a:90–97

Brodholt J, Stein S. 1988. Rheological control

Annu. Rev. Earth Planet. Sci. 1995.23:169-213. Downloaded from www.annualreviews.org by California Institute of Technology on 06/20/13. For personal use only.

of Wadati-Benioff zone seismicity. *Geophys. Res. Lett.* 15:1081–84

Burnley PC. 1990. *The effect of nonhydrostatic stress on the olivine-spinel transformation in Mg_2GeO_4*. PhD dissertation. Univ. Calif., Davis

Burnley PC, Green HW II, Prior D. 1991. Faulting associated with the olivine to spinel transformation in Mg_2GeO_4 and its implications for deep-focus earthquakes. *J. Geophys. Res.* 96:425–43

Burnley PC, Green HW II. 1989. Stress dependence of the mechanism of the olivine-spinel transformation. *Nature* 338:753–56

Bussod GY, Katsura T, Sharp TG. 1994. A view into the Earth's transition zone: experimental deformation of β-$Mg_{1.8}Fe_{0.2}SiO_4$ at high pressures and high temperatures. *TERRA Nova 6:* Abs. Suppl. 1:9 (Abstr.)

Chung W, Kanamori H. 1980. Variation of seismic source parameters and stress drops within a descending slab and its implications in plate mechanics. *Phys. Earth Planet. Inter.* 23:134–59

Coe RS, Kirby SH. 1975. The orthoenstatite to clinoenstatite transformation by shearing and reversion by annealing: mechanism and potential applications. *Contrib. Mineral. Petrol.* 52:29–55

Dupas C, Doukhan N, Doukhan J-C, Green HW II, Young TE. 1994. Analytical electron microscopy of a synthetic peridotite experimentally deformed in the β olivine stability field. *J. Geophys. Res.* In press

Engebretson D, Kirby S. 1992. Deep Nazca slab seismicity: why is it so anomalous? *Eos, Trans. Am. Geophys. Union* 73:379 (Abstr.)

Evison FF. 1963. Earthquakes and faults. *Bull. Seismol. Soc. Am.* 53:873–91

Evison FF. 1967. On the occurrence of volume change at the earthquake source. *Bull. Seismol. Soc. Am.* 57:9–25

Fletcher RC, Pollard DD. 1981. Anticrack model for pressure solution surfaces. *Geology* 9:419–24

Frohlich C. 1987. Aftershocks and temporal clustering of deep earthquakes. *J. Geophys. Res.*

Frohlich C. 1989. The nature of deep-focus earthquakes. *Annu. Rev. Earth Planet. Sci.* 17:227–54

Fukao Y, Kikuchi M. 1987. Source retrieval for mantle earthquakes by iterative deconvolution of long-period *P*-waves. *Tectonophysics* 144:249–69

Fukao Y, Obayashi M, Inoue H, Nenbai M. 1992. Subducting slabs stagnant in the mantle transition zone. *J. Geophys. Res.* 97(B4):4809–22

Giardini D. 1988. Frequency distribution and quantification of deep earthquakes. *J. Geophys. Res.* 93:2095–105

Gilbert F, Dziewonski AM. 1975. An application of normal mode theory to the retrieval of structural parameters and source mechanisms from seismic spectra. *Philos. Trans. R. Soc. London. Ser. A* 278:187–269

Gillis KM, et al. 1993. A view of the lower crustal component of hydrothermal systems at the Mid-Atlantic Ridge. *J. Geophys. Res.* 98:19,597–619

Glennon MA, Chen W-P. 1994. Ruptures of deep-focus earthquakes in the northwestern Pacific and their implications on seismogenesis. *Geophys. J. Int.* In press

Goto K, Suzuki Z, Hamaguchi H. 1987. Stress distribution due to olivine-spinel phase transition in descending plate and deep focus earthquakes. *J. Geophys. Res.* 92:13,811–20

Grand SP. 1994. Mantle shear structure beneath the Americas and surrounding oceans. *J. Geophys. Res.* 99:11,591–622

Green HW II. 1984. How and why does olivine transform to spinel? *Geophys. Res. Lett.* 11:817–20

Green HW II. 1986. Phase transformation under stress and volume transfer creep. In *Mineral and Rock Deformation: Laboratory Studies,* Geophys. Monogr. Ser. Vol. 36, ed. B Hobbs, H Heard, pp. 201–13. Washington, DC: Am. Geophys. Union

Green HW II. 1992. Analysis of deformation in geological materials. In *Minerals and Reactions at the Atomic Scale: Transmission Electron Microscopy,* ed. PR Buseck. *Rev. Mineral.* 27:425–54

Green HW II, Burnley PC. 1989. A new, self-organizing, mechanism for deep-focus earthquakes. *Nature* 341:733–37

Green HW II, Burnley PC. 1990. The failure mechanism for deep-focus earthquakes. In *Deformation Mechanisms. Rheology and Tectonics,* ed. RI Knipe, EM Rutter, 54:133–41. London: Geol. Soc. Spec. Publ.

Green HW II, Scholz CH, Tingle TN, Young TE, Koczynski TA. 1992a. Acoustic emissions produced by anticrack faulting during the olivine → spinel transformation. *Geophys. Res. Lett.* 19:789–92

Green HW II, Young TE, Walker D, Scholz CH. 1990. Anticrack-associated faulting at very high pressure in natural olivine. *Nature* 348:720–22

Green HW II, Young TE, Walker D, Scholz CH. 1992b. The effect of nonhydrostatic stress on the $\alpha \rightarrow \beta$ and $\alpha \rightarrow \gamma$ olivine phase transformations. In *High-Pressure Research: Application to Earth and Planetary Sciences,* ed. Y Syono, MH Manghnani, Geophys. Monogr. 67, pp. 229–35. Tokyo: Terra Sci.; Washington, DC: Am. Geophys. Union

Green HW II, Zhou Y. 1994. Transformation-induced faulting and the cessation of earthquakes at 680 km depth. *Tectonophysics.* Submitted

Griggs DT. 1954. High-pressure phenomena

Annu. Rev. Earth Planet. Sci. 1995.23:169-213. Downloaded from www.annualreviews.org by California Institute of Technology on 06/20/13. For personal use only.

with applications to geophysics. In *Modern Physics for the Engineer,* ed. LN Ridenour, pp. 272–305. New York: McGraw-Hill

Griggs DT. 1972. The sinking lithosphere and the focal mechanism of deep earthquakes. In *The Nature of the Solid Earth,* ed. EC Robertson, pp. 361–84. New York: McGraw-Hill

Griggs DT, Baker DW. 1969. The origin of deep-focus earthquakes. In *Properties of Matter Under Unusual Conditions,* ed. H Mark, S Fernbach, pp. 23–42. New York: Wiley Interscience

Griggs DT, Handin JH. 1960. Observations on fracture and a hypothesis of earthquakes. In *Rock Deformation,* ed. DT Griggs, JH Handin. *Mem. Geol. Soc. Am.* 79:347–73

Hasegawa A, Umino N, Takagi A. 1978. Double-planed deep seismic zone and upper mantle structure in the northeastern Japan arc. *Geophys. J. R. Astron. Soc.* 54:281–96

Hasagawa A, Zhao D, Hori S, Yamamoto A, Horiuchi S. 1991. Deep structure of the northeastern Japan arc and its relationship to seismic and volcanic activity. *Nature* 352:683–89

Helffrich G, Brodholt J. 1991. Relationship of deep seismicity to the thermal structure of subducted lithosphere. *Nature* 353:252–55

Helffrich G, Stein S, Wood BJ. 1989. Subduction zone thermal structure and mineralogy and their relationship to seismic wave reflections and conversions at the slab/mantle interface. *J. Geophys. Res.* 94(B1):753–63

Hobbs BE, Ord A. 1988. Plastic instabilities: implications for the origin of intermediate and deep focus earthquakes. *J. Geophys. Res.* 93:10,521–40

Hodder APW. 1984. Thermodynamic constraints on phase changes as earthquake source mechanisms in subduction zones. *Phys. Earth Planet. Inter.* 34:221–25

Houston H. 1993. The non-double-couple component of deep earthquakes and the width of the seismogenic zone. *Geophys. Res. Lett.* 16:1687–90

Houston H, Vidale J. 1994. The temporal distribution of seismic radiation during deep earthquake rupture. *Science* 265:771–74

Houston H, Williams Q. 1991. Fast rise times and physical mechanism of deep earthquakes. *Nature* 352:520–22

Houston H, Zhang J. 1992. A global survey of the state of stress in subducting slabs: the role of phase transformations. *Proc. Wadati Conf. Great Subduction Earthquakes,* ed. D Christensen, M Wyss, RE Habermann, J Davies, pp. 37–38. Fairbanks: Geophys. Inst. Univ. Alaska

Iidaka T, Furukawa Y. 1994. Doubleseismic zone for deep earthquakes in the Izu-Bonin subduction zone. *Science* 263:1116–18

Iidaka T, Suetsugu D. 1992. Seismological evidence for metastable olivine inside a subducting slab. *Nature* 356:593–95

Isacks B, Molnar P. 1971. Distribution of stresses in the descending lithosphere from a global survey of focal-mechanism solutions of mantle earthquakes. *Rev. Geophys. Space Phys.* 9:103–74

Jeffreys H. 1929. *The Earth. Its Origin, History and Physical Constitution.* Cambridge, UK: Cambridge Univ. Press. 2nd ed.

Jeffreys H. 1936. The structure of the Earth down to the 20° discontinuity. *Proc. R. Soc. Edinburgh* 56:158–63

Kanamori H, Allen CR. 1986. Earthquake repeat time and average stress drop. In *Earth Source Mechanics,* Geophys. Monogr., ed. S Das, J Boatwright, CH Scholz, 37:227–35. Washington, DC: Am. Geophys. Union

Kao H, Chen W-P. 1994. The double seismic zone in Kuril-Kamchatka: the tale of two overlapping single seismic zones. *J. Geophys. Res.* 99:6913–30

Katsura T, Ito E. 1989. The system Mg_2SiO_4-Fe_2SiO_4 at high pressures and temperatures: precise determinations of stabilities of olivine, modified spinel and spinel. *J. Geophys. Res.* 94:15,663–70

Kawakatsu H. 1986. Downdip tensional earthquakes beneath the Tonga arc: a double seismic zone? *J. Geophys. Res.* 91:6432–40

Kawakatsu H. 1991. Insignificant isotropic component in the moment tensor of deep earthquakes. *Nature* 351:50–53

Kirby SH. 1987. Localized polymorphic phase transformation in high-pressure faults and applications to the physical mechanism of deep focus earthquakes. *J. Geophys. Res.* 92:13, 789–800

Kirby SH, Durham WB, Stern L. 1991. Mantle phase changes and deep earthquake faulting in subducting lithosphere. *Science* 252:216–25

Kuge K, Kawakatsu H. 1993. Significance of non-double couple components of deep and intermediate-depth earthquakes: implications from moment tensor inversions of long-period seismic waves. *Phys. Earth Planet. Inter.* 75:243–66

Lay T. 1994a. The fate of descending slabs. *Annu. Rev. Earth Planet. Sci.* 22:33–61

Lay T. 1994b. Seismological constraints on the velocity structure and fate of subducting lithospheric slabs: 25 years of progress. *Adv. Geophys.* 35:1–185

Lieberman RC. 1975. Elasticity of olivine, beta and spinel polymorphs of germanates and silicates. *Geophys. J. R. Astron. Soc.* 42:899–929

Liebertz J, Rooymans CJM. 1965. The ilmenite/perovskite phase transformation of $CdTiO_3$ under high pressure. *J. Phys. Chem.* 44:242–49 (In German)

Liu L. 1983. Phase transformations, earthquakes and the descending lithosphere. *Phys. Earth Planet. Inter.* 32:226–40

Lockner DA, Byerlee JD, Kuksenko V, Pono-

marev A, Sidorin A. 1991. Quasi-static fault growth and shear fracture energy in granite. *Nature* 350:39–42

Lockner DA, Byerlee JD, Kuksenko V, Ponomarev A, Sidorin A. 1992. Observations of quasistatic fault growth from acoustic emissions. In *Fault Mechanics and Transport Properties of Rocks,* ed. B Evans, TF Wong, pp. 3–31. London: Academic

Lundgren PR, Giardini D. 1992. Seismicity, shear failure and modes of deformation in deep subduction zones. *Phys. Earth Planet. Inter.* 74:63–74

Matsuzawa T, Kono T, Hasegawa A, Takagi A. 1990. Subducting plate boundary beneath the northeastern Japan arc estimated from SP converted waves. *Tectonophysics* 181:123–33

Meade C, Jeanloz R. 1989. Acoustic emissions and shear instabilities during phase transformation in Si and Ge at ultrahigh pressure. *Nature* 339:616–18

Meade C, Jeanloz R. 1991. Deep-focus earthquakes and recycling of water into the Earth's mantle. *Science* 252:68–72

Mikumo T. 1971. Source process of deep and intermediate earthquakes as inferred from long period *P* and *S* waveforms. 2. Deep-focus and intermediate-depth earthquakes around Japan. *J. Phys. Earth* 19:303–20

Morris J, Tera F. 1989. ^{10}Be and ^{9}Be in mineral separates and whole rocks from volcanic arcs: implications for sediment subduction. *Geochim. Cosmochim. Acta* 53:3197–206

Mukherjee AK, Bieler TR, Chokshi AH. 1989. Superplasticity in metals and ceramics. *Proc. 10th Riso Int. Symp. on Metallurgy and Materials Science: Materials Architecture,* ed. JB Bilde-Sorensen, pp. 207–31. Roskilde, Denmark: Riso Nat. Lab.

Navrotsky A, Bose K. 1994. Hydrous phases may be stable into the transition zone. *Eos, Trans. Am. Geophys. Union,* Spring Meet. Suppl. 99:230

Nehlig P, Juteau T, Bendel V, Cotton J. 1994. The root zones of oceanic hydrothermal systems: constraints from the Semail ophiolite (Oman). *J. Geophys. Res.* 99:4703–13

Ogawa M. 1987. Shear instability in a viscoelastic material as the cause of deep focus earthquakes. *J. Geophys. Res.* 92:13,801–10

Okal EA, Geller RJ. 1979. On the observability of isotropic sources: the July 31, 1970 Colombian earthquake. *Phys. Earth Planet. Inter.* 18:176–96

Okal EA, Kirby SH. 1993. Deep earthquakes beneath the North Fiji Basin: faulting in a detached and recumbant slab transforming from metastable peridotite to the slab transition-zone mineral assemblage? *Eos, Trans. Am. Geophys. Union,* Fall Meet. Suppl. 98:97

Okal EA, Kirby SH, Stein S. 1993. The onset of deep earthquakes in the Indonesia subduction zone: relationship to slab thermal maturity and mantle phase changes. *Eos, Trans. Am. Geophys. Union,* Spring Meet. Suppl. 98:309

Orowan E. 1960. Mechanism of seismic faulting. In *Deformation,* ed. DT Griggs, J Handlin, 79:323–45. London: Geol. Soc. Memoir

Pacalo REG, Gasparik T. 1990. Reversals of the orthoenstatite-clinoenstatite transition at high pressures and high temperatures. *J. Geophys. Res.* 95:15,853–58

Petit JP, Barquins M. 1988. Can natural faults propagate under mode II conditions? *Tectonics* 7: 1243–56

Post RL Jr. 1977. High temperature creep of Mt. Burnet dunite. *Tectonophysics* 42:75–110

Raleigh CB, Paterson MS. 1965. Experimental deformation of serpentinite and its tectonic implications. *J. Geophys. Res.* 70:3965–85

Richter FM. 1979. Focal mechanisms and seismic energy release of deep and intermediate earthquakes in the Tonga-Kermadec region and their bearing on the depth extent of mantle flow. *J. Geophys. Res.* 84:6783–95

Ross N, Navrotski A. 1987. The Mg_2GeO_4 olivine-spinel phase transformation. *Phys. Chem. Mineral.* 14:473–81

Rubie DC. 1993. Mechanisms and kinetics of reconstructive phase transformations in the Earth's mantle. In *Short Course Handbook on Experiments at High Pressure and Applications to the Earth's Mantle,* ed. RW Luth, pp. 247–303. Edmonton: Mineral. Assoc. Can.

Rubie DC, Ross CR II. 1994. Kinetics of the olivine-spinel transformation in subducting lithosphere: experimental constraints and implications for deep slab processes. *Phys. Earth Planet. Inter.* 86:223–41

Rubie DC, Tsuchidat Y, Yagi T, Utsumi W, Kikegawa T, et al. 1990. An in situ X ray diffraction study of the kinetics of the Ni_2SiO_4 olivine-spinel transformation. *J. Geophys. Res.* 95:15, 829–44

Ryan JG, Langmuir CH. 1993. The systematics of boron abundances in young volcanic rocks. *Geochim. Cosmochim. Acta* 57:1489–98

Sakuyama M. 1983. Phenocryst assemblages and H_2O content in circumPacific arc magmas. In *Geodynamics of the Western Pacific and Indonesian Regions,* ed. TWC Hilde, S Uyeda, pp. 143–58. Washington, DC: Am. Geophys. Union

Scholz CH. 1989. Mechanics of faulting. *Annu. Rev. Earth Planet. Sci.* 17:309–34

Scholz CH. 1990. *The Mechanics of Earthquakes and Faulting.* Cambridge, UK: Cambridge Univ. Press

Stein CA, Stein S. 1992. A model for the global variation in oceanic depth and heatflow with lithospheric age. *Nature* 359:123–29

Stolper EM, Newman S. 1994. The role of water in the petrogenesis of Mariana trough magmas. *Earth Planet. Sci. Lett.* 293–325

Sung CM. 1979. Kinetics of the olivine-spinel

Annu. Rev. Earth Planet. Sci. 1995.23:169-213. Downloaded from www.annualreviews.org by California Institute of Technology on 06/20/13. For personal use only.

transition under high pressure and temperature: experimental results and geophysical implications. In *High-Pressure Science and Technology*, ed KD Timmerhaus, MS Barber, pp. 31–41. New York: Plenum

Sung CM, Burns RG. 1976. Kinetics of the olivine-spinel transition: implications to deep-focus earthquake genesis. *Earth Planet. Sci. Lett.* 32:165–70

Sykes LR. 1966. The seismicity and deep structure of island arcs. *J. Geophys. Res.* 71:298–326

Tatsumi Y, Hamilton DL, Nesbitt RW. 1986. Chemical characteristics of fluid phase released from a subducted lithosphere and origin of arc magmas: evidence from high-pressure experiments and natural rocks. *J. Volcanol. Geotherm. Res.* 29:293–309

Thompson AB. 1992. Water in the Earth's upper mantle. *Nature* 358:295–302

Tingle TN, Green HW, Borch RS. 1991. High temperature creep experiments on the olivine and spinel polymorphs of Mg_2GeO_4: implications for the rheology of the Earth's mantle. *Eos, Trans. Am. Geophys. Union* 72:297 (Abstr.)

Tingle N, Green HW II, Scholz CH, Koczynski TA. 1993. The rheology of faults triggered by the olivine-spinel transformation in Mg_2GeO_4 and its implications for the mechanism of deep-focus earthquakes. *J. Struct. Geol.* 15:1249–56

Turner HH. 1922. On the arrival of earthquake waves at the antipodes, and on the measurement of the focal depth of an earthquake. *Mon. Not. R. Astron. Soc. Geophys. Suppl.* 1:1–13

Vaisnys JR, Pilbeam CC. 1976. Deep-earthquake initiation by phase transformation. *J. Geophys. Res.* 81:985–88

van der Hilst R, Engdahl R, Spakman W, Nolet G. 1991. Tomographic imaging of subducted lithosphere below northwest Pacific island arcs. *Nature* 353:37–43

Vassiliou MS, Hager BH, Raefsky AR. 1984. The distribution of earthquakes with depth and stress in subducting slabs. *J. Geodyn.* 1:11–28

Vaughan PJ, Coe RS. 1981. Creep mechanism in Mg_2GeO_4: effects of a phase transition. *J. Geophys. Res.* 86:389–404

Vaughan PJ, Green HW II, Coe RS. 1984. Anisotropic growth in the olivine-spinel transformation of Mg_2GeO_4 undernonhydrostatic stress. *Tectonophysics* 108:299–322

Vidale JE, Benz HM. 1992. Upper-mantle seismic discontinuities and the thermal structure of subduction zones. *Nature* 356:678–83

Vidale JE, Houston H. 1993. The depth dependence of earthquake duration and implications for rupture mechanisms. *Nature* 365:45–47

Vidale JE, Williams Q, Houston H. 1991. Waveform effects of a metastable olivine tongue in subducting slabs. *Geophys. Res. Lett.* 18:2201–4

Wadati K. 1928. Shallow and deep earthquakes. *Geophys. Mac.* 1:162–202

Wiens DA, McGuire JJ, Shore PJ. 1993. Evidence for transformational faulting from a deep double seismic zone in Tonga. *Nature* 364:790–93

Wyss M, Molnar P. 1972. Source parameters of intermediate and deep focus earthquakes in the Tonga arc. *Phys. Earth Planet. Inter.* 6:279–92

Zhao D, Sacks IS. 1994. Metastable phase change mechanism for deep earthquakes: a seismological constraint. *Eos, Trans. Am. Geophys. Union*, Spring Meet. Suppl. 99:234

Zhou HW. 1990. Observations on earthquake stress axes and seismic morphology of deep slabs. *Geophys. J. Int.* 103:377–401

Annu. Rev. Earth Planet. Sci. 1995.23:169-213. Downloaded from www.annualreviews.org by California Institute of Technology on 06/20/13. For personal use only.